Optimized design method for storage systems in photovoltaic plants with delivery limitation

Antonio Colmenar-Santos[1,*], Mario Monteagudo-Mencucci[1], Enrique Rosales-Asensio[2], Miguel de Simón-Martín[2] and Clara Pérez-Molina[1]

[1]Department of Electric, Electronics, Control, Telematics and Applied Chemestry Engineering, UNED
Juan del Rosal, 12 – Ciudad Universitaria
28040 Madrid, Spain
[2]Department of Electric, Systems and Automatics Engineering, Universidad de León
Campus de Vegazana s/n
24071 León, Spain

*Corresponding author. Tel.: +34 913 987 788; fax: +34 913 986 028.
E-mail addresses: acolmenar@ieec.uned.es (Antonio Colmenar-Santos), mmonteagu29@alumno.uned.es (Mario Monteagudo-Mencucci), arosa@unileon.es (Enrique Rosales-Asensio), miguel.simon@unileon.es (Miguel de Simón-Martín), clarapm@ieec.uned.es (Clara Pérez-Molina).

Abstract— **It results widely common for distribution network operators to impose restrictions on delivered solar photovoltaic generated power when the power plant rated power is greater than the maximum allowed due to the distribution network capacity. Thus, a feasible solution to maximize the performance of the solar power plant is the integration of battery energy storage systems. Although this configuration has been extensively studied in the existing literature, an optimal design method to determine the proper size and operation of the energy storage system needs to be developed. In this paper, a novel method to help power plants designers to determine the optimal battery energy storage capacity to integrate into any solar photovoltaic power plant is provided. The proposed algorithm minimizes the potential power curtailment and optimizes the utilization rate of the batteries storage system. The algorithm can be applied to any grid connected solar photovoltaic power plant under delivery power restrictions, regardless of power capacity and location. The algorithm has been implemented to a simulated power plant with delivery limitations based in a real case, and results with the optimal battery capacity show that the system would be able to recover up to the 83% of the curtailed energy and a yearly average capacity utilization of 56%. Moreover, the BESS operation has been validated with a scaled model run in Simulink and laboratory measurements, achieving 98% of curtailed energy recovery rate and a 57% of average capacity utilization.**

Keywords: Renewable energy storage; Photovoltaic solar energy; System optimization; Battery capacity.

NOMENCLATURE

AC	Alternating Current.
Ah	Ampere per hour current capacity.
BESS	Battery Energy Storage System.
C	BESS capacity value [kWh].
C_{opt}	Optimal BESS capacity value [kWh].
$C_{achievement}\ (C,L)$	Average annual capacity utilization rate (it depends on C and L) [-].
$C_{delivered}(C,L)$	Specific delivered energy recovered from the BESS (it depends on C and L) [kWh/kW].
$C_{extra}(C,L)$	Annual extra recovered energy coefficient (it depends on C and L) [-].
CPI	Consumer Price Index [%].
d	Number of days considered to compute $C_{achievement}$ [days].
DNO	Distribution Network Operator.
DC	Direct Current.
$E_{extra}(L)$	Annual total curtailed energy (it depends on L) [kWh].
$E_{delivered}(L)$	Annual total recovered energy from the BESS (it depends on C and L) [kWh].
$f(C,L_t)$	Target function to optimize (it depends on C and L) [-].
HV	High voltage.
IRR	Internal Rate of Return [%].
IGBT	Insulated gate bipolar transistor.
kW	Kilowatt.
kWh	Kilowatt per hour.
L	Power curtailment due to power grid restrictions [kW].
LCOE	Levelized Cost of Energy.
ms	Millisecond.
µs	Microsecond.
MPPT	Maximum Power Point Tracker.
MW	Megawatt.
n	Number of pairs of cut-off points which define the curtailment periods [-].
n'	Number of pairs of cut-off points which define the BESS discharging periods [-].
PoC	Point of Connection (grid border).
PPC	Power Plant Controller.
$P_{ch}(t)$	Required charge power for the BESS (it depends on t) [kW].
$P_{disch}(t)$	Discharge power for the BESS (it depends on t) [kW].
$P_{PV}(t)$	Solar photovoltaic power generation potential without limitations (it depends on t) [kW].
PR	Performance ratio [%].
PV	Photovoltaic.
RES	Renewable Energy Source.
SG	Smart Grid.
S	Sulphur.
SoC (C,L,t)	State of Charge (it depends on C, L and t) [%].
SoC_{min}	Minimum allowed State of Charge for the BESS [%].
SoC_{max}	Maximum allowed State of Charge for the BESS [%].
T_{sample}	Integration time step used in the simulation [s].
VBA	Visual Basic programming language.
V2G	Vehicle to grid.
V_{dc}	Direct current voltage.
Wp	Watt peak power.
η_{ch}	BESS charging efficiency [-].
η_{disch}	BESS discharging efficiency [-].

1. INTRODUCTION

Due to the progressively higher penetration of renewable energy sources (RES) in the distribution network, Distribution Network Operators (DNOs) have recently been forced to address major technical challenges. One of the most remarkable problems is the appearance of large amounts of uncontrolled, difficult-to-forecast and highly dependent on local conditions, energy injections in the distribution network. Thus, a common practice of DNOs is to limit the rated power of grid connected power plants to a 50 percent of the technical capacity of the network to which the plant is to be connected [1]. In the case of solar photovoltaic (PV) power plants, their rated power is associated with their peak power, which occurs under standard conditions (defined by horizontal irradiance value of 1,000 W/m^2, ambient temperature of 25 ºC and air mass value of 1.5), which are usually achieved only under clear sky conditions and an small daily time window. Then, these power plants are used to be clearly oversized and show very low performance ratios, high curtailment rates and low yearly equivalent hours (ratio between the yearly generated energy and the yearly energy that could be produced working continuously at the rated power).

Therefore, power plant owners and promotors have been considering the incorporation of battery energy storage systems, or BESS, in PV power plants in order to oversize the power plant capacity while complying with the technical limitations imposed by the DSOs; and storing the potential power plant's surplus energy during periods of maximum production in order to deliver it to the power grid during low irradiance periods. However, it is still unclear how to define the appropriate size of the BESS in order to guarantee the profitability of the energy storage as it is characterized, by the moment, by high investment costs and considerable operation and maintenance needs. Thus, the authors in this paper propose a novel method for designing the storage capacity of the BESS integrated in a PV power plant (or other uncontrolled, variable resource fed power plant) with power delivery limitations, with the aim of maximizing the ratio of the surplus energy injected into the grid (or in other words, minimizing the curtailment ratio) while maximizing the use of the installed energy storage capacity; this means maximizing the amount of energy per MWh installed in the BESS, which will ultimately be related to the plant's economic profitability.

Electrical storage technology can be seen from two different points of view: independent distributed storage and centralized storage. The former combined with smart grids (SG) points to have good possibilities, considering that it has aroused interest in the scientific community, as shown by the number of publications based on the use of electric or hybrid vehicles, connected to the standby distribution network through V2G (Vehicle to grid) technologies and, thus, converting into a large virtual distributed electricity storage system, and also the recent investments that private companies are performing in this technology. Moreover, some studies depict new possibilities with standalone systems integrated in heterogeneous cellular networks [2]. The analysis of the advantages and drawbacks of the former versus the latter approach is likewise of interest [3]. Furthermore, management of system controllers is also important in the former approach [4]. In [5] and [6], the use of V2G combined with PV is considered to limit consumption peaks in a SG, seeking to minimize the power consumption from the external power grid and prioritizing the energy generated via the PV system. Another approach worth to be mentioned is the use of BESS in hybrid systems; e.g., in [7] an off-grid photovoltaic hybridized with a diesel generator and a BESS is analysed, providing a new energy management algorithm; in [8] a smart sizing approach is provided for a photovoltaic fed water pumping system. In this work, it has been exclusively considered the latter approach because the goal in this work is the *ad hoc* design of a BESS in the specific case of power delivery limitations and provide an optimisation method easily implemented in commonly PV design software by VBA scripts. Then, the curtailment minimization and the maximization of the average BESS capacity utilization are used as designing criteria. Moreover, real operation conditions of the proposed BESS have been simulated by scaling an equivalent *Simulink*® model, validating this way the proposed method. Fig. 1 summarizes in a graphic scheme the proposed approach.

This paper is organized as follows. In next section, the solar PV generation potential model is presented. Then, the behaviour of the power plant is analysed and the expressions to obtain the optimal value of C for the BESS are

presented. The algorithm has been coded in VBA scripts which are provided in the Supplementary material. In the third section, the conditions of the plant where the study will be carried out are defined, as well as the simulation conditions where the simulation will provide the data for the development of the design method. For this purpose, a simulation based on a real plant is carried out using the *PVsyst*® and weather data from *Meteonorm*® [9]. The Simulations and Results section shows the simulation configuration and the obtained results by implementing the proposed BESS optimization method. First simulations set works with a real 10 MVA solar PV power plant data and the analysis are conducted in *Microsoft Excel*®. Then, a second simulations set is conducted in *Simulink*® [10] in order to assess the operation behaviour of the BESS. Due to computing limitations, the *Simulink*® model corresponds to a scaled PV power plant which conditions has been replicated in the laboratory. While the first set of simulations work with a complete year data, the second set has been applied only to three reference days, corresponding to three irradiation conditions: low, average and high irradiation. Moreover, this last set of simulations in *Simulink*® have been conducted under three BESS size scenarios: (i) considering the optimal BESS capacity size, (ii) considering the double of the optimal BESS size, and (iii) considering the half of the optimal BESS size. Finally, the results are analysed in the Discussion section and conclusions, further research lines and advantages and disadvantages of the proposed approach are included in the last section. An appendix section has been included with the *Simulink*® simulation graphical results.

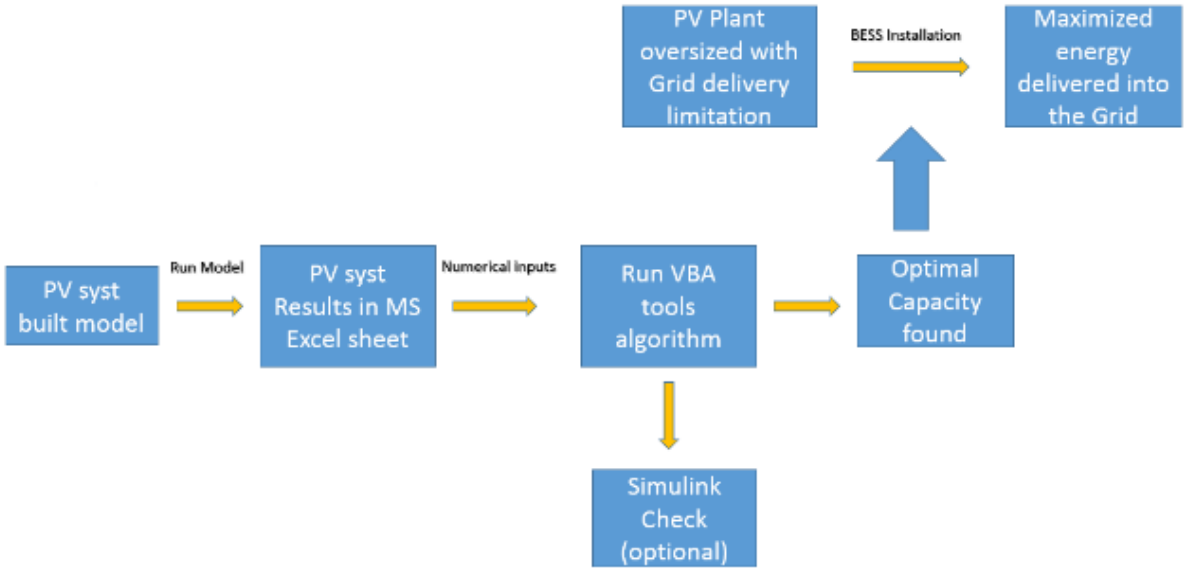

Fig. 1. Block diagram of the proposed method for BESS capacity sizing optimization. Source: own elaboration.

2. THEORETICAL BACKGROUND

Numerous papers have been published on storage systems in solar plants in recent years [11], [12], [13] and [14]. Part of this research is devoted to developing control systems that optimize the use of batteries in networks with high PV penetration [15], or integral management for PV systems, BESS and load forecast with hourly rate [16]. A great deal of research has been conducted into the use of BESS with the aim of mitigating and/or eliminating contingencies in DNOs for particular cases [17] and for commercial networks [18], in order to peak load shaving, power curve smoothing and voltage regulation in transformer distribution networks, a BESS is evaluated to obtain such goals in [19]. Techno-economic analysis of a PV/Biomass/fuel cell energy is presented in [20] and a standalone roof top PV system with BESS is analysed in [21]. Other researches are focused in different solar technologies cost optimization as in [22], where base structural design for cylindrical reflector system is presented. In line with the scope of this paper, algorithms have also been designed for optimizing the use of PV + ESS systems, penalizing client peak consumption. The primary aim of these algorithms is to maximize customer benefits with PV avoiding returns

of power, while the second is to improve the load profile by modifying customer consumption behaviours [23]. Also, in [24] customer consumption behaviours are evaluated with BESS installation, faced to a consumption behaviour without BESS. However, none of these papers include the design of an optimized sizing method for the capacity of the system to be installed. In [25], a control strategy is defined for the integration of PV + BESS in DC microgrids. Three scenarios are considered: connected to the grid, isolated, and transition. The strategy coordinates in the same scenario the BESS, PV, load management, and SoC in isolated mode. In AC mode, AC/DC inverters are used to stabilize the system by conducting, as in this paper, *Simulink*® simulations—using the DC voltage level as the input parameter to the control system. Some management systems include adaptive-predictive mechanisms with expert domains [26], which will be discussed in the final section of this paper devoted to future research focused on BESS management in PV plants. Authors in [27] define an energy management system based on a predictive model controller of an isolated hybrid system where PV energy systems, wind power, a fuel cell, and a BESS system are involved. There are reports showing predictive systems on management of battery combined with PV systems improves the IRR of the installation, this is the same case of study published in [28] and [29] were a PV system with BESS installation is optimized with financial approach, considering economic conditions. The novelty of this paper provides a tool to determine the capacity of the system that optimizes its exploitation, something that is not provided on other research. The followed procedure in this work, only the main values of the BESS system have been considered, such as the storage capacity in kWh or the state of charge. The authors consider this is the best way to address the capacity without depending on the direct current voltage (V_{dc}), as is the case when it is expressed in hourly amps (Ah), charge and discharge power, and time periods. The *Simulink*® simulation has considered the battery technology used. It is hence necessary to obtain an accurate enough battery model. Although it does not necessarily mean it is the most optimal technology from an economic point of view, a Li-ion battery was thus chosen. A detailed review of the different existing electrical energy storage technologies (including batteries and different technologies) can be found in [30], where it is shown that the technology based on NaS is the most widely used in BESS, followed by Lead Acid, Li-ion, and Ni-Cd. However, there are reports that shows that Pb-acid technology presents a better economic cost/energy production ratio compared to NaS technology. In [31] an overview on recent development in ESS is presented.

Authors in [32] have carried out a batteries' size optimization sought following a Markov-Chains approach for a number of technologies. The use of batteries can reduce the variability. In [33], a statistical model is employed to find the optimal configuration for a BESS based on batteries and supercapacitors. Furthermore, authors in [34] provide a developed method for BESS optimization within an installation in which all elements are connected to the AC bus, using DC-AC inverters for the PV plant and AC-DC/DC-AC inverters for the BESS. The developed method seeks the economic optimization of the operation with the facilities for the very specific case in which there are two tariff periods, the objective function being the minimization of the cost function. The work fully describes the mathematical formulation employed in the procedure. This procedure provides a capacity value for maximum values of energy delivered into the grid, however this doesn't mean it will result in an improvement in the economic cost. This is not the case of this research, where a general approach for all possible configurations are considered in terms of systems but only in the case of PV plants on grid connected with limited export capacity. Not always the research works are focused in the AC bus, in [35], a research is developed to optimize a microgrid operation at DC bus level.

Given that the scope of this paper is to analyse the optimized design of BESS, it should be pointed out that, although different papers have been published in this respect, to the best of our knowledge none of them has provided tools for a design to be applied in PV plants with power delivery limitation. Although a BESS sizing method is provided in [36], it focuses on reducing the power returns to the DNO point of connection (PoC) and also on countering the overload in the transformers of the companies [this method is tested using Monte Carlo based simulations]. Barsali et al. show in [37] the results of two years of experimentation with BESS. It analyses the technical and economic benefits of an energy storage system made up of equipment employing different technologies. On the other hand, in [38], Zalani et al. develop a BESS control algorithm to obtain a smoothed output PV power production curve; results

are employed to obtain the payback time of the BESS. Different researches focus on the instant compensation of the energy generated by RES systems with the power load, seeking to minimize imbalances in the grid caused by the increase in PV penetration in the distribution systems, as it is required by regulations in markets such as those of Germany [39], Spain [40], Italy [41], and the UK [42]. Finally, in [43], a BESS is studied focusing on minimizing the difference between the PV production estimation and actual production.

In general terms, current scientific contributions regarding the optimal sizing of BESS show pure economic or technical approaches. Nevertheless, it also can be found specific works where particular technical issues, such as power ramps limitations (these sorts of limitations can result mandatory in some power systems, e.g., the case of regulations in Puerto Rico [44]), limitations of frequency band deflections by power returns [45], reactive power compensation, overhead distribution transformers or primary frequency control of islanded microgrids [46] are considered.

3. MATERIALS AND METHODS

3.1 PV generation potential model

In this work, the optimal sizing of a BESS coupled to a PV power plant with power delivery limitations is proposed. Then, power generation potential is estimated through advanced simulation software fed with weather and climate files and characteristics of the desired power plant components. Real generated power data can be optionally used to validate the results if they are available (usually they can be gathered from the monitoring platforms deployed in this sort of facilities). In order to perform the simulations in this work, daily climate data files from *Meteonorm*® have been used.

Once that the climate data files are obtained for the desired location of the PV power plant, hourly electricity generation without limitations must be estimated accurately. There exist several methods to conduct this sort of simulations, from the simplest to the most accurate and complex. Several PV power estimation software can be found, both private or open source. One of the most widely used for its reliability and accurate results is *PVsyst*®, which is characterized because it offers hourly power estimations and results can be exported to spreadsheets (such as *Microsoft Excel*®) and other software data file formats.

Hourly PV power estimations are discrete data. In order to reduce data size and improve energy calculations by integration methods, polynomial regression techniques are applied. Thus, based on the data provided by the PV power estimation software (*PVsyst*®), 6th grade polynomial equations have been adjusted for each daily power profile, according to equation (1).

$$P_{PV}^{i}(t)=a_{i,0}+a_{i,1}\cdot t^{1}+a_{i,2}\cdot t^{2}+a_{i,3}\cdot t^{3}+a_{i,4}\cdot t^{4}+a_{i,5}\cdot t^{5}+a_{i,6}\cdot t^{6}, \quad (1)$$

where $P_{PV}^{i}(t)$ is the estimated hourly PV power generation [kW] for daytime t [h], and for the i-th day of a natural year, with $i \in \{1,2,\ldots,365\}$. $a_{i,j}$ is the j-th coefficient [-] of the 6th grade polynomial.

The polynomial adjustment through the least-squares method can be easily implemented in a *Microsoft Excel*® spreadsheet by simply using the function:

$$\text{LINEST}(m_1;m_2\text{^}\{1;2;3;4;5;6\};1;0), \quad (2)$$

where m_1 is the matrix of values to be estimated while m_2 is the matrix with the polynomial coefficients to be estimated. The last two terms in the function specify they are independent variable terms and if adjustment deviations statistics are desired to be provided, respectively.

One of the main advantages of computing the polynomial regression through a software, such as *Microsoft Excel*® is that the polynomial calculation for each day can be automated through Visual Basic (VBA) programmed routines (in supplementary material chapter A, polynomial calculation code in VBA is provided).

Figs. 2 and 3 show the comparison of the discrete simulation data values and the estimations with the obtained polynomial functions. Only a clear (Fig. 2) and a cloudy (Fig. 3) are shown as examples. It can be observed that the proposed approach is highly accurate, especially for clear sky conditions. Although some discrepancies can be observed in cloudy days, the proposed polynomial degree is enough to provide good results for the method.

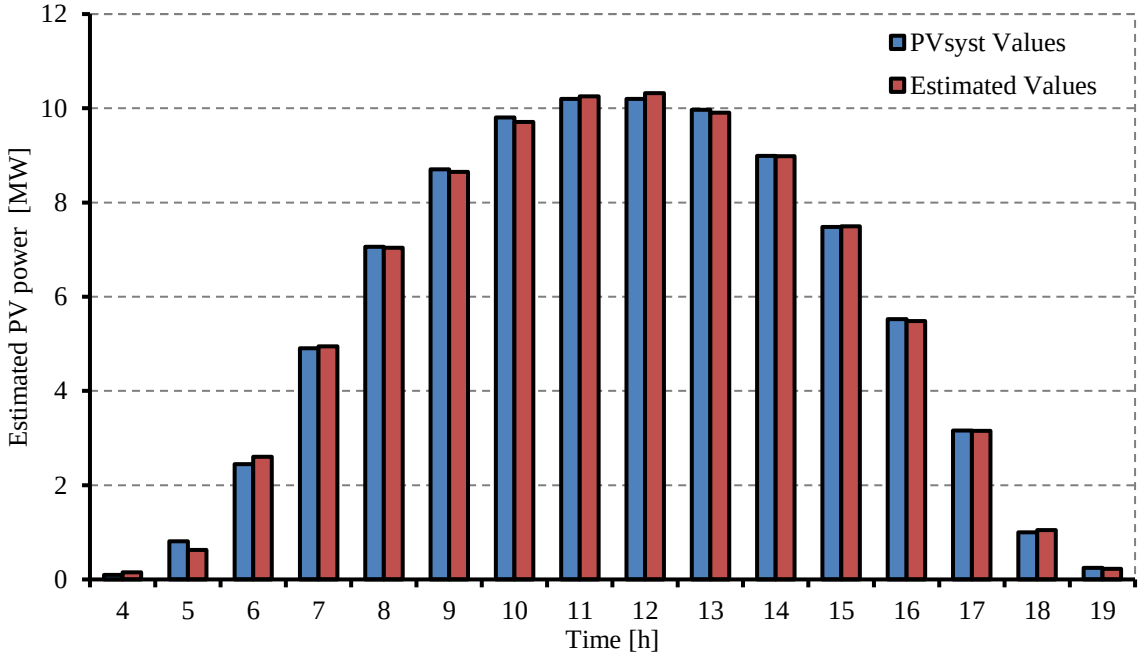

Fig. 2. Simulated and polynomic approximations of PV generated power under clear sky conditions. Source: own elaboration.

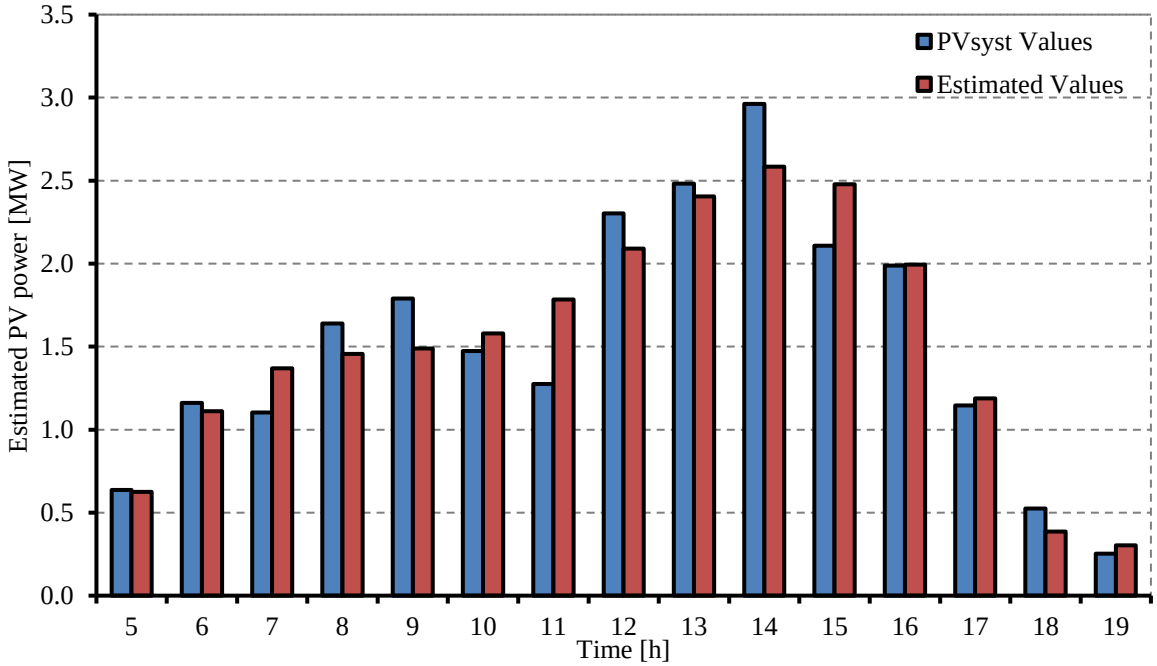

Fig. 3. Simulated and polynomic approximations of PV generated power under cloudy conditions. Source: own elaboration.

With the daily power curves calculated before, energy calculations can be easily performed for any desired time window. Fig. 4 shows the estimated monthly PV generated energy by the plant under study, considering no energy delivery limitations.

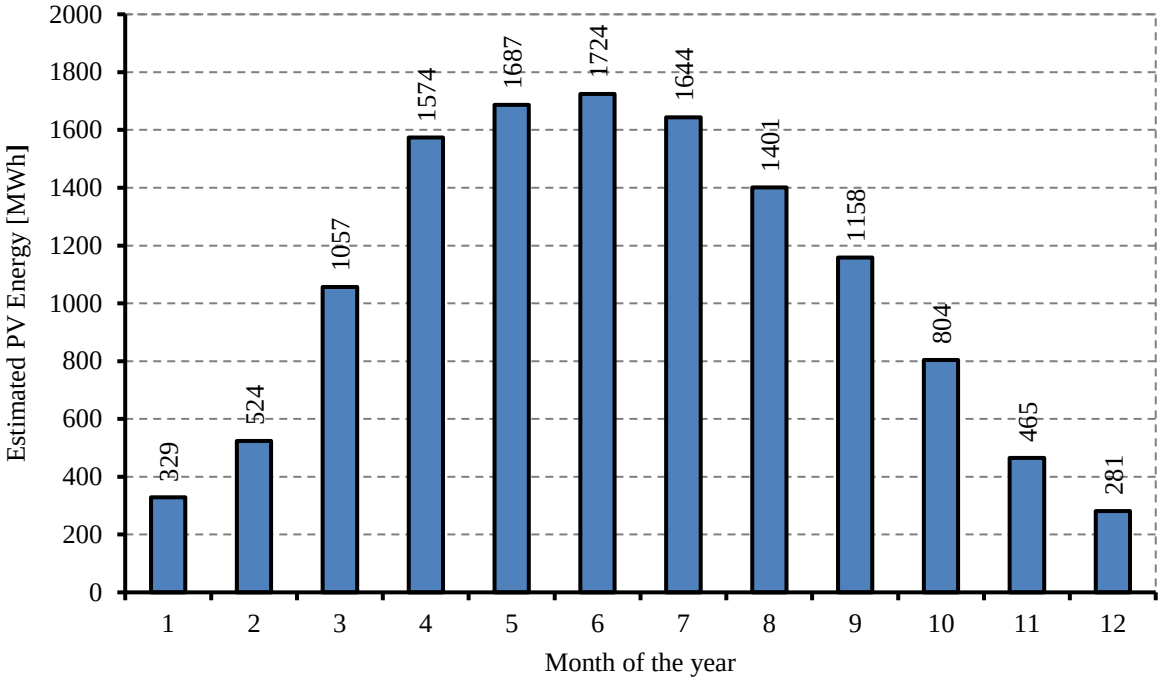

Fig. 4. Estimated monthly PV energy generation without delivery limitations. Source: own elaboration.

Comparing the total annual energy productions of the *PVsyst*® results and those from the polynomic regression, a percentage difference less than 10^{-9} between both results is obtained. Thus, the overall fit of annual production is considered good enough and the PV generation potential model is validated.

3.2 Calculation of the optimal BESS size

To optimize the BESS installed capacity size (C_{opt}) a target function is defined. This target function can be defined in technical, economic terms, or both. Although other specific targets can be found applying the proposed method, in this case, it results mandatory to minimize the power curtailment due to delivery limitations and maximize the BESS profit through its average daily utilization.

The power curtailment (energy that could be produced by the generation system but that it could not be delivered to the power grid) can be quantified as shown in equation (3).

$$P_{extra}(P_{PV},L) = P_{PV} - L, \forall P_{PV} \geq L, \tag{3}$$

where P_{extra} [kW] is the power curtailment due to the maximum power delivery limitation, L [kW] and P_{PV} is the solar photovoltaic power which would be generated without limitations [kW], defined in equation (1).

However, depending on the installed BESS capacity, the real curtailed and then delivered energy[1], $E_{delivered}$ [kWh], can differ from the total curtailed energy, E_{extra}, defined in equation (10). Then, the C_{extra} value [-] is defined as the ratio between the real delivered energy recovered thanks to the installed BESS and the total curtailed energy,

[1] Due to the charging and discharging efficiency rates are lower than 1, $E_{delivered}$ only considers the final delivered energy into the power grid.

as shown in equation (4).

$$C_{extra}(C, L) = \frac{E_{delivered}(C,L)}{E_{extra}(L)}, \quad (4)$$

where $E_{delivered}$ corresponds with the additional amount of energy that the PV power plant have been able to export into the power grid after the installation of the BESS, i.e. the yearly energy that the BESS delivers into the grid.

On the other hand, in order to see the utilisation of the BESS, it is advised to express $E_{delivered}$ in specific terms:

$$C_{delivered}(C, L) = \frac{E_{delivered}(C,L)}{C}, \quad (5)$$

where $C_{delivered}(C, L)$ is the specific energy [kWh/kW] that can be delivered additionally to the power grid because it has been stored under delivery limitation conditions and it was injected when PV production was lower than the power limitation and C is the BESS capacity [kW].

Let's notice that the $C_{delivered}(C, L)$ value is strictly decreasing when C increases. As soon as C is increased, the annual energy production also increases, but not in the same proportion as in the first installed MWh. This effect appears because as the capacity increases, it also does the underutilization rate, which is especially significant on cloudy days in PV power plants. Thus, the daily average utilization of the BESS capacity should be considered for optimization purposes. That value is considered in this work with the $C_{achievement}(C, L)$ variable, which depends on the BESS installed capacity. This parameter is calculated as the average daily ratio of the energy storage in the BESS system and the installed capacity, as it is shown in equation (6), where d is the number of days in the analysis period (typically one natural year or 365 days). In an optimal design, $C_{achievement}(C, L)$ must be maximum, as it is related with maximum economic profit and minimum levelized cost of energy (LCOE). The proposed algorithm to calculate the $C_{achievement}(C,L)$ value is provided in supplementary material Chapter F.

$$C_{achievement}(C, L) = \frac{1}{d}\sum_{i=1}^{d} C_{delivered}^{i}(C, L). \quad (6)$$

To combine both targets, a multi-target optimization approach must be considered. Although several techniques could be applied, such as the calculation of Pareto fronts, a simple but effective method has been implemented in this case, which simply consists of defining the target function, f(C, L), as the product of both targets, as both must be maximized [see equation (7)]. This approach allows fast calculations and optimal performance.

$$f(C,L) = C_{achievement}(C,L) \cdot C_{extra}(C,L), \quad (7)$$

To the target function seen in equation (7), two constraints must be added defining the upper and lower limits for the BESS installed capacity C. As optimization method, several approaches can be applied. In this work the SIMPLEX optimization solver is proposed, as it results efficient for solving this linear programming (LP) optimization problem, that can be implemented in a *Microsoft Excel*® spreadsheet through the provided *"Solver"* toolkit. Genetic optimization algorithms can also be applied, if desired, through the *"Evolutionary"* solver.

As final remark, C_{opt} [kWh] will be the BESS capacity size value that arranges the optimal value for f(C, L).

3.3 Determination of the curtailed and delivered energy

Both the E_{extra} and $E_{delivered}$ values must be computed to perform the BESS optimization. In the case of E_{extra}, the area above the power delivery limitation, L, must be calculated. It should be noticed that this area may exist or not in a daily period and, in the case there exist curtailment, this situation may occur several times. At any case, the number of cut-off points must be an even number. An example with two curtailment situations can be observed in Fig. 5, where the power delivery limitation has been set at 7 MW.

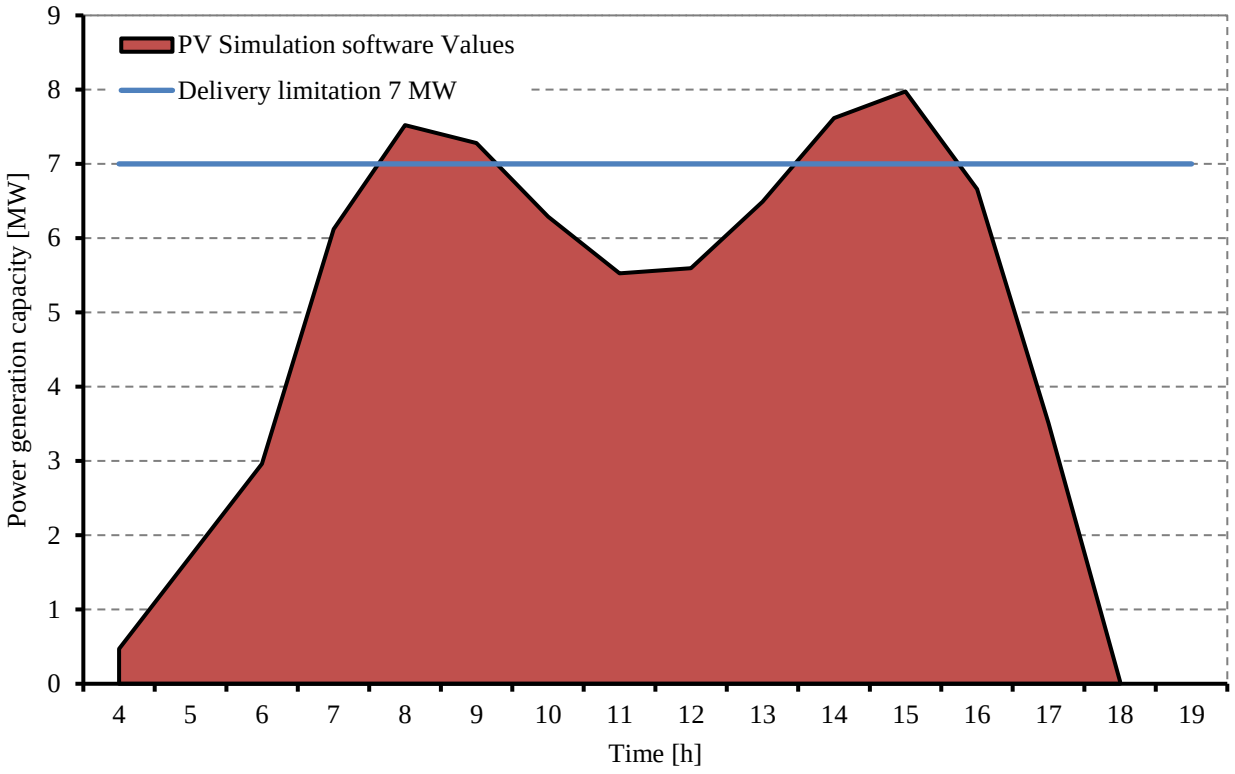

Fig. 5. Example of a daily profile with curtailment due to maximum power delivery. Source: own elaboration.

The algorithm must be able to find and obtain all the pairs of cut-off points and discriminate between valleys and peaks in order to, accordingly, calculate the battery charge in the peaks (if the BESS has available capacity), or battery discharge in the valleys (if the BESS has available power load).

Cut-off points are those that satisfy the following expression:

$$P_{PV}^{i}(t) - L = 0, \tag{8}$$

where i is the analysed day of the year. To find all possible solutions for equation (8), when they exist, a solver tool with a local search region (giving to the search a resolution of 0.1) has been implemented and it is provided in supplementary material Chapters B and C.

To compute the $E_{extra}(L)$ value for each day, equation (9) was implemented in a VBA script that is executed for each daily profile and that can be found in Chapter D of the supplementary material:

$$E_{extra}^{i}(L) = \sum_{j=1}^{2n-1} \int_{t_j}^{t_{j+1}} \left[P_{PV}^{i}(t) - L\right] \mathrm{d}t, \tag{9}$$

where n is the number of pairs of cut-off points which define the curtailment intervals found on the i-th day, t_j [h] the start cut-off point of the j-th curtailment interval and t_{j+1} [h] the end cut-off point of the interval. Then, the total annual curtailed energy can be calculated according to equation (11).

$$E_{extra}(L) = \sum_{i=1}^{365} E_{extra}^{i}(L). \tag{10}$$

The provided VBA script can be executed with the command *"Extra_Energy"* which takes just a single argument: the power delivery limitation (L). Furthermore, let's notice that the calculated cut-off points are also displayed in the default cells from the calculation spreadsheet.

On the other hand, in order to compute the $E_{delivered}$ value for each analysed day, the following considerations must be considered:

i. The battery is considered initially fully discharged (BESS State of Charge, SoC, at minimum level).
ii. The BESS must absorb all the available surplus energy until full capacity is reached or the generated power gets lower than the power delivery limitation (see Fig. 6).
iii. If a power curve valley is observed during the day, the battery must be discharged at a power rate satisfying the power delivery limitation, while the SoC is greater than the minimum or until the power delivery limitation is reached (see Fig. 6).

The charging and discharging equations are shown in expressions (11) and (12) respectively:

$$P_{ch}(C,L,t)=\begin{cases}\eta_{ch}[P_{PV}(t)-L] & if\ \mathrm{SoC}(C,L,t)\leq \mathrm{SoC}_{max}\\ 0 & otherwise\end{cases}, \quad (11)$$

$$P_{disch}(C,L,t)=\begin{cases}\eta_{disch}[L-P_{PV}(t)] & if\ \mathrm{SoC}(C,L,t)\geq \mathrm{SoC}_{min}\\ 0 & otherwise\end{cases}, \quad (12)$$

where $P_{ch}(C,L,t)$ is the charging power [kW], η_{ch} the charging efficiency [-], $P_{disch}(C,L,t)$ is the discharging power [kW] and η_{disch} the discharging efficiency [-]. SoC_{min} and SoC_{max} are the minimum and maximum States of Charge [%] allowed for the BESS. Then, the BESS state of charge is computed as:

$$\mathrm{SoC}\,(C,L,t)=\mathrm{SoC}\,(C,L,t-1)+\frac{\int P_{ch}(C,L,t)\mathrm{d}t}{C}-\frac{\int P_{disch}(C,L,t)\mathrm{d}t}{C}, \quad (13)$$

and the energy delivered to the power grid thanks to the BESS in an analysis period of d days (one natural year) can be calculated as shown in equation (14).

$$E_{delivered}(C,L)=\sum_{i=1}^{d}E^{i}_{delivered}(C,L)=\sum_{i=1}^{d}\left(\sum_{j=1}^{2n'-1}\int_{t_j}^{t_{j+1}}P_{disch}(C,L,t)\mathrm{d}t\right), \quad (14)$$

where n' is the number of pairs of discharging cut-off points for the i-th day of analysis. The proposed algorithm to solve the $E_{delivered}$ value is shown in supplementary material Chapter E.

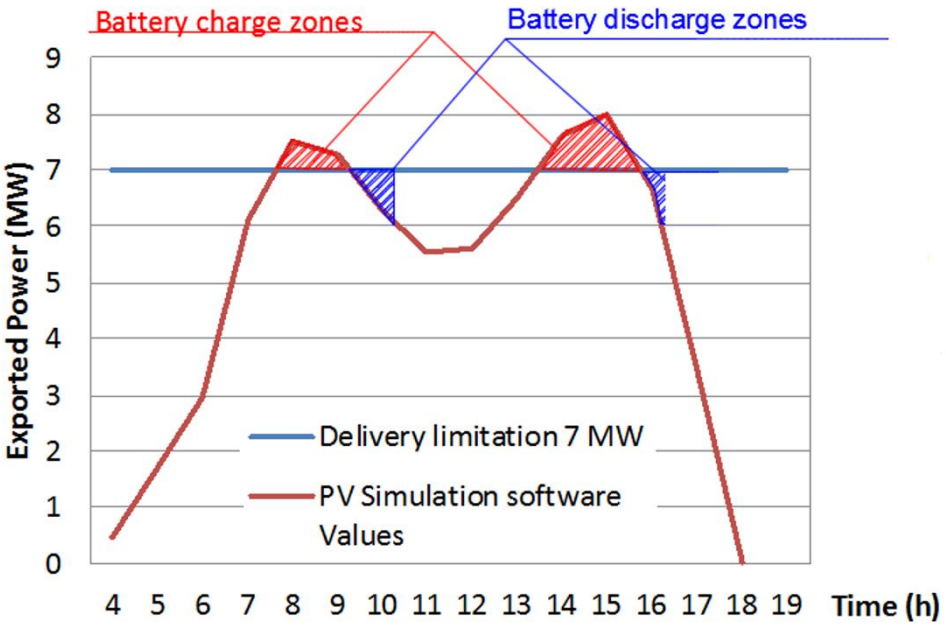

Fig. 6. BESS operation. Source: own elaboration.

4. SIMULATION AND RESULTS

In this section, a real PV power plant has been simulated and the proposed BESS optimal sizing approach has been applied. Both the power plant operating conditions and the simulation results are provided, comparing the three possible scenarios: without BESS and power delivery limitation, without BESS but with power delivery limitation and with optimized BESS and power delivery limitation. Furthermore, the actual production data provided by the plant monitoring system is analysed and compared with the simulations to validate the model.

4.1 Power plant description and simulation conditions

The study was carried out at a large-scale photovoltaic power plant placed in the UK. This plant has a total peak power of 12 MWp distributed in 2,047 series of 23 panels of 255 Wp each, manufactured in polycrystalline silicon and consisting of 60 cells. The chosen orientation was azimuth 0, the tilt of panels 20° with the horizontal plane, and the mounting structure is fixed type.

The plant has four 1,350 kW rated power PV inverters and three 1,200 kW rated power PV inverters, constituting a 9 MW nominal power plant. The maximum AC power delivered by each inverter is 1,530 kVA and 1,360 kVA, respectively. Therefore, the total maximum AC power delivered by the power plant is 10.2 MVA. The plant is also provided with a transformer substation in order to fit the generation voltage level to the grid voltage level. In order to concentrate the total amount of power generated by the plant at the PoC, a high voltage customer substation has been built in which the HV power lines coming from the plant transformer substations will be connected. In Fig. 7 it is shown the PV plant layout under study, showing PV panels in blue areas, inverter stations pink coloured, roads and the main access to the PV plant. In order to connect the plant to the distribution grid, a company substation has been built where high-voltage protection switchgear has been installed prior to delivering the power to the distribution grid. The PoC will be at 33 kV.

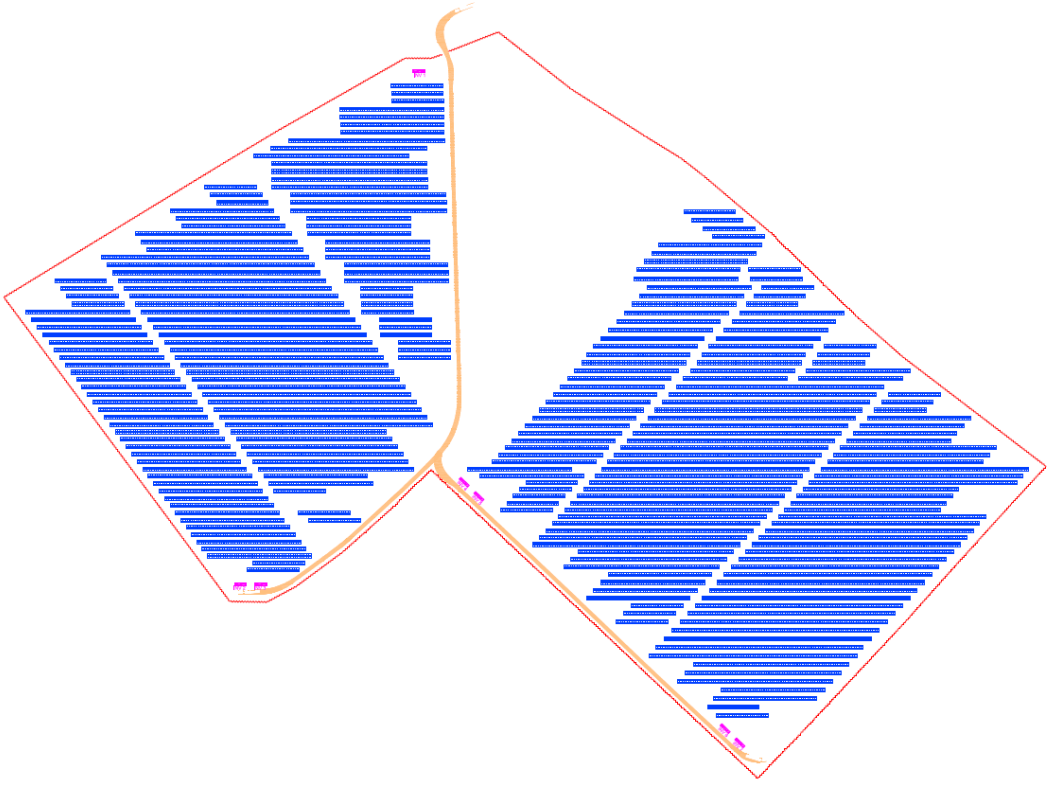

Fig. 7. Layout of the PV plant subject to the analysis. Source: own elaboration.

For running the sizing and operation simulations, the *Meteonorm*® 97 [49] database was used for this purpose, where the main data, as hourly radiation, temperature, sun position (height and azimuth) and wind speed are provided for each single day. These data are the basis of calculation to estimate the PV generation of the plant.

The profile of nearby obstacles on which the shadow loss diagram is based, including architectural elements, panels, vegetation, etc., was defined. A detailed calculation of the shading losses of the plant was likewise carried out. Fig. 8 shows the layout window used for the calculation, where the grey areas mean the PV panels over ground mounted system (simulation of projected shadows over adjacent panels) and the green areas show the generated shadows by hedges and vegetation.

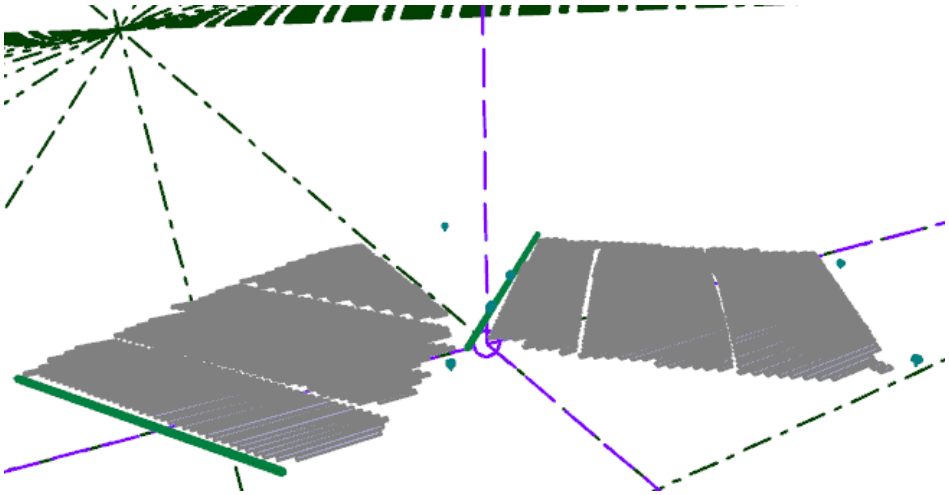

Fig. 8. Layout of the shadows calculation in *PVsyst*® simulation software. Source: own elaboration.

The PV production estimation has been performed through *PVsyst*® software. The characteristics of the installed PV modules are defined by *".PAN"* file provided by the manufacturer and extracted data from datasheets provided in [50], where it has been considered the efficiency of the commercial panels as per the manufacturer specifications, considering the different temperatures and operation environment conditions. The strings configuration is defined in this case by two arrays corresponding to each of the two types of inverters installed in the plant. The two installed inverters were likewise defined by the provided *".OND"* file by the inverter manufacturer. Moreover, in the simulation, all efficiency factors affecting the global system has been considered, including, but not limited to, mismatching, soil and ohm effect losses.

The simulation was performed in two scenarios, with power delivery limitation and without it, in order to compare the difference between the two results for the developed optimization procedure.

4.2 Power plant simulation without BESS integration

The PV plant operating without any power delivery limitation and with no BESS installed capacity is able to generate a total annual production of 12,464 MWh with a performance ratio (PR) of 85.09% and a specific (or normalized) yield production of 1,038 $kWh \cdot kWp^{-1} \cdot year^{-1}$ is obtained. Fig. 9 (a) shows the average monthly normalized production.

On the other hand, setting a power delivery limitation of 7.5 MW, the total annual production is reduced to 12,043 MWh, with a performance ratio (PR) of 82.22% and a specific yield production of 1,003 $kWh \cdot kWp^{-1} \cdot year^{-1}$. Fig. 9 (b) shows the average monthly normalized production in this scenario.

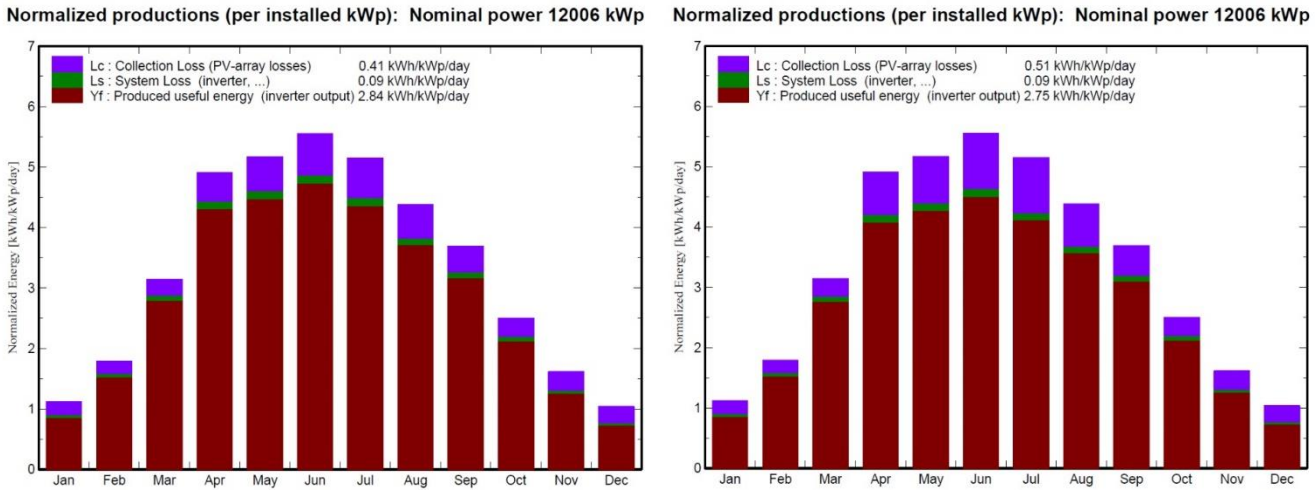

(a) (b)

Fig. 9. Average monthly normalized PV generation of the power plant (a) without power delivery limitation and (b) with power delivery limitation of 7.5 MW. Source: own elaboration.

4.3 BESS sizing and simulation

Due to special power load profiles and the existence of other generators in the distribution grid where the presented PV power plant is connected, the distribution company grants a maximum output power of 7.5 MVA, which is less than the maximum 10 MVA AC that the plant is available to produce. Thus, the plant is currently operating with its inverters limited to the maximum this power delivery limitation and a significant amount of energy is being curtailed. The installation of a BESS is hence required to absorb the surplus energy at peak periods to be delivered later. Then, the following design criteria must be fulfilled:

1. To prevent in any case whatsoever the PV plant from delivering a higher power than the established maximum limitation.

2. When the battery system has sufficient capacity and the PV plant is producing above 7.5 MVA, the difference must be accumulated in the storage system.

3. When the difference between the maximum authorized power and the power generated by the plant is positive, the BESS must start to deliver the accumulated energy at the admissible power value.

4. If the plant exceeds the maximum authorized power and the BESS reaches 100% SoC, the inverters will adjust their operating curve to their limits.

5. In the case of charging the BESS, if the power generated by the power plant minus the maximum authorized power exceeds the maximum charge power of the BESS, the inverters will self-regulate to maintain the charge power of the BESS within limits.

The BESS equipment was supplied by the BYD company [47] and comprised two containers each of 12.2 metres, with a maximum power charge per container of 1 MW and a capacity of 1 MWh. Moreover, a 2 MVA dry transformer would also be installed to connect the BESS to the substation bus, which would deliver the power from the battery plant to the grid and would consume the power sent from the PV plant to the battery. On the other hand, a power plant controller (PPC) was installed to provide the settings to each inverter according to the analysis of operation that the system carries out at every instant at the plant (from a network analyser installed in a customer

substation busbar) and the signals it receives from the BYD BESS communications system [48]. To obtain the signals from each inverter, the plant has been provided with a fibre optic network to link the PPC with each inverter unit.

First, to validate the BESS model, real installed BESS capacity (2 MWh) has been simulated and compared with real measurements from the power plant monitoring platform. Results are shown in Fig. 10. In this figure, except March, it can be observed quite similar results between simulation values and real measurements, which validates the presented model. Differences found for March are due to downtimes in the power plant as result of the BESS configuration. In annual terms, the difference of the energy delivered from the BESS between simulated values and real measurements is just 24.83 MWh·year^{-1}, which means a deviation lower than 6% with the simulated curtailed energy (420.933 MWh·year^{-1}).

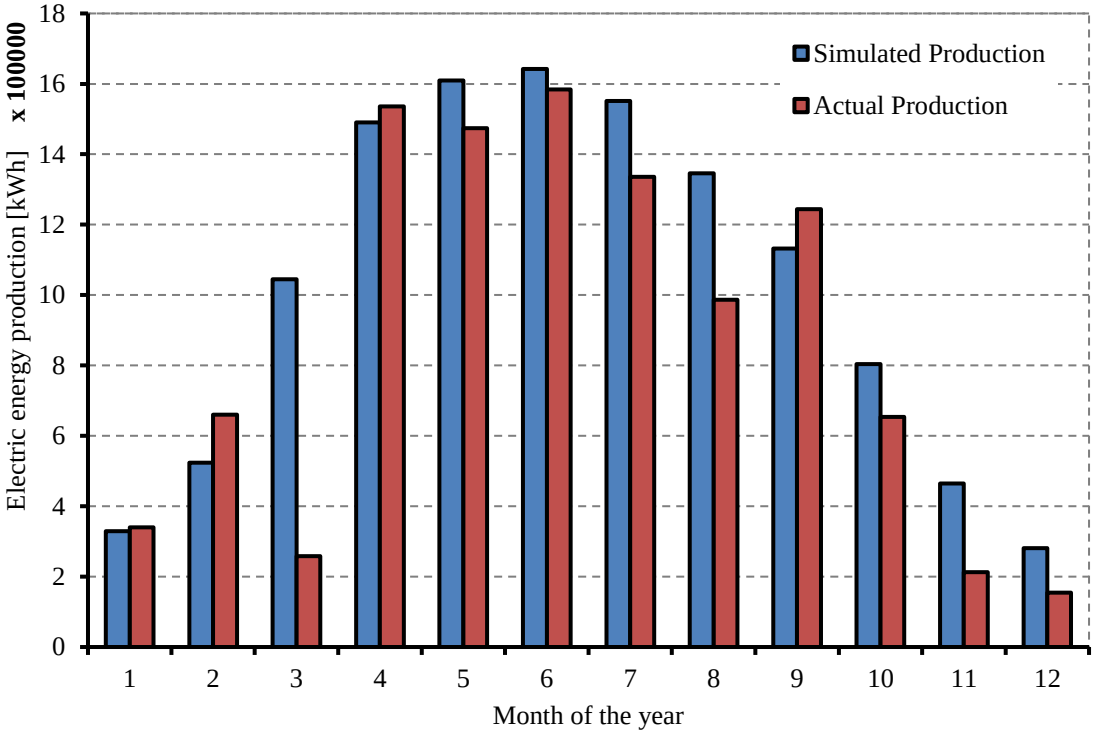

Fig. 10. Comparison between simulated results and real measurements for 2 MWh BESS installed capacity. Source: own elaboration.

Applying the proposed method, described in the previous section, to the PV power plant under study, an optimal BESS capacity value of C_{opt} = 6,655.352 kWh is obtained. It can be observed in Fig. 11 the evolution of the target function f(C,L) with the proposed BESS capacity C, and how an installed capacity value of C_{opt} maximizes this function {max[f(C,L)]=0.4617}. Let's notice that this proposed optimal value triples the intended value of 2 MWh.

Table 1 summarizes the $C_{extra}(C,L)$ and the $C_{achievement}(C,L)$ values for both BESS installed capacities (intended and optimized). It can be seen that, although a 2 MWh of installed capacity shows a better $C_{achievement}(C,L)$ value, the corresponding $C_{extra}(C,L)$ value is significantly lower, which means an equivalent reduction in economic income.

Table 1. Parameters evaluation for intended and optimized BESS installed capacity. Source: own elaboration.

BESS capacity C [MWh]	**$C_{achievement}$ [%]**	**C_{extra} [%]**
2.00	84.11	37.30
6.66	56.00	82.81

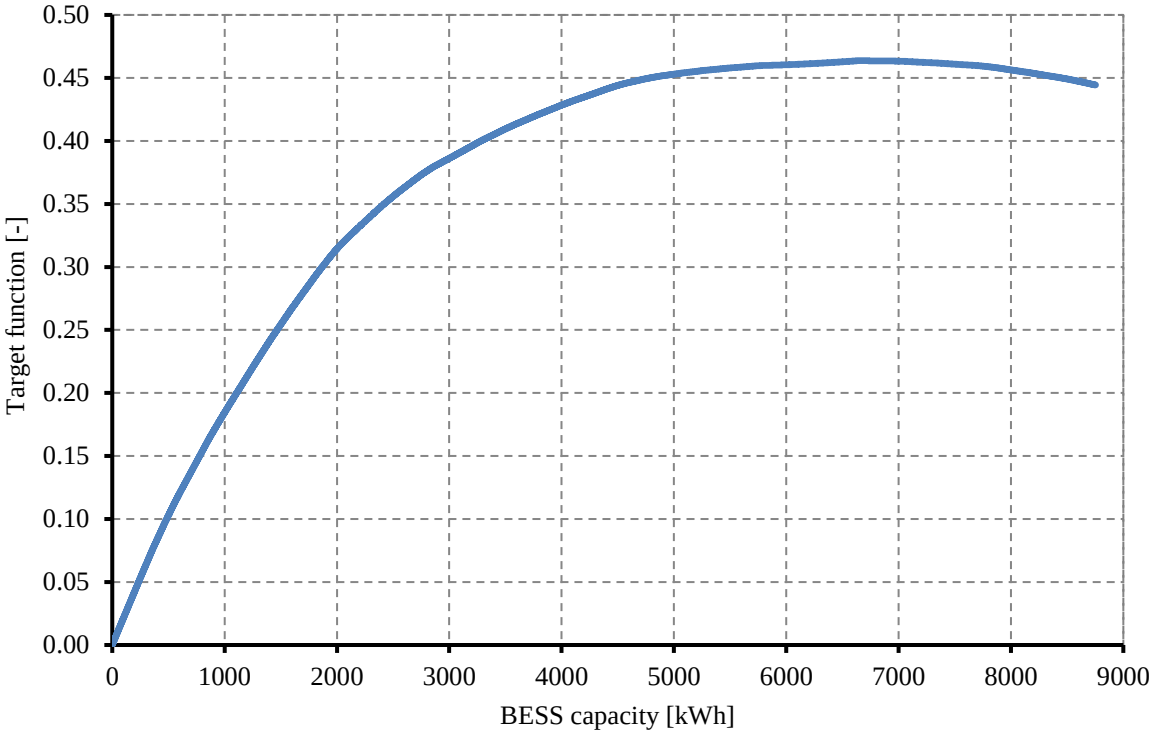

Fig. 11. Target function evolution with the BESS installed capacity. Source: own elaboration.

From an economical point of view, considering the hypotheses that (i) the PV power plant can be operated 25 years (common value for their useful lifespan), (ii) the Consumer Price Index (CPI) is set at 3%, (iii) the yearly growing rate of the electricity price can be considered at 5%, (iv) the price of the installed capacity in a BESS can be approximated to the Pb-acid technology, estimated in 120 $/kWh [51], and (v) given the average cost of electricity of 0.145 $/kWh; the economic analysis is presented in Table 2.

Table 2. Economic analysis of the BESS installation with optimal size. Source: own elaboration.

Energy delivered [kWh·year^{-1}]	**Cost of BESS [$]**	**Incomings [$·year^{-1}]**	**IRR [%]**	**Pay-back [years]**	**NPV [$]**
348,574.62	798,600.00	50,543.32	7.49	13.35	1,194,354.00

As it can be seen in Table 2, the optimal BESS sizing allows to obtain a pay-back time less than 14 years and an IRR of almost 7.5%, which is considered reasonable in the RES field.

4.4 Validation of the operation strategy

Finally, the aptitude of the BESS operation strategy has been simulated by using a *Simulink*® equivalent model. The aim of this test is to check the installed capacity behaviour under different scenarios and validate if the calculated C_{opt} really optimizes the power plant operation.

Simulating a PV power plant with the size characteristics like the one under study, would need long time periods of simulation as well as large computation resources. Due to the limitations in simulation time, temporary and size equivalents are established in such a way the simulation steps have been adjusted to a reasonable computation time. Then, a scaled model has been implemented. Thus, the developed model in *Simulink*® consists of a single-phase inverter with an incremental conductance MPPT integral controller, according to [52]. A PV array consisting of three strings of 7 panels model Trina Solar TSM 260 PD05, with 260 Wp peak power have been considered [53]. As inverter, a Solar River 6000 TL US Samil Power inverter was considered [54]. It is important to note that, while the

default inverter used in PV *Simulink*® models is a standard one, it has been tunned similar enough to the Solar River 6000 TL US Samil Power inverter to validate the results regarding the BESS capacity. The resulting installed modules power was 5.45 kWp in a 5 kW inverter group. Accordingly, a value of 2 kW was considered as power delivery limitation. Fig. 12 shows both the characteristic curves of the PV modules [subfigure (a)] and the power inverter [subfigure (b)]. While de characteristic curves of the PV modules represent the output power of the module with the voltage, the characteristic curves of the power inverter represent the efficiency depending on the working load. It should be noticed that the power output of the PV modules depends directly on the solar irradiance, being the reference conditions, the standard conditions (with 1,000 $W \cdot m^{-2}$ of incident solar global irradiance). On the other hand, the power inverter efficiency depends on the voltage (210 V, 380 V and 500 V efficiency curves are provided) and maximum power conversion efficiency (around 97%) is provided in this model when the power load is the 60% of the inverter's rated power.

Fig. 13 show the current and power curves of the simulated PV field and their variation with the PV cell temperature (the higher the PV cell temperature, the lower the output voltage and power). MPPT algorithms are mandatory to make the PV field work at maximum power by regulating its voltage.

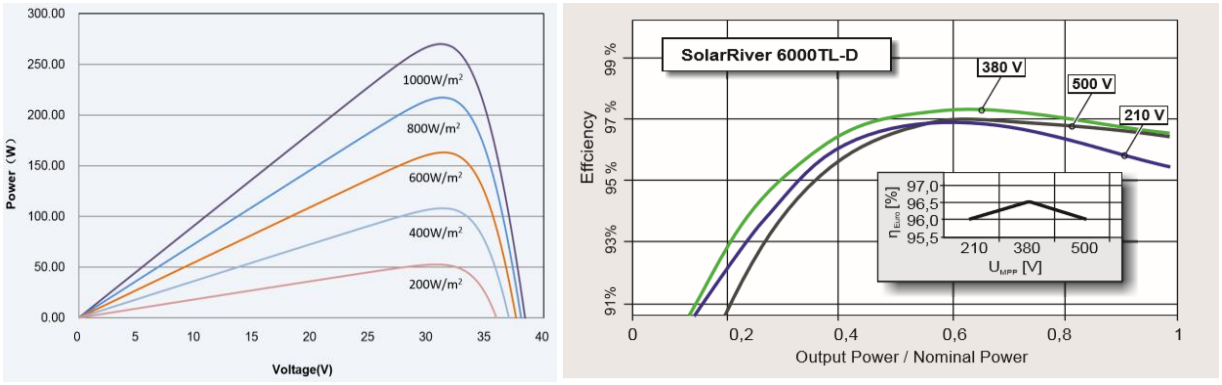

(a) (b)

Fig. 12. Characteristic curves of (a) the solar PV module and (b) the power inverter. Sources: Trina Solar Limited and Samil Power Co.

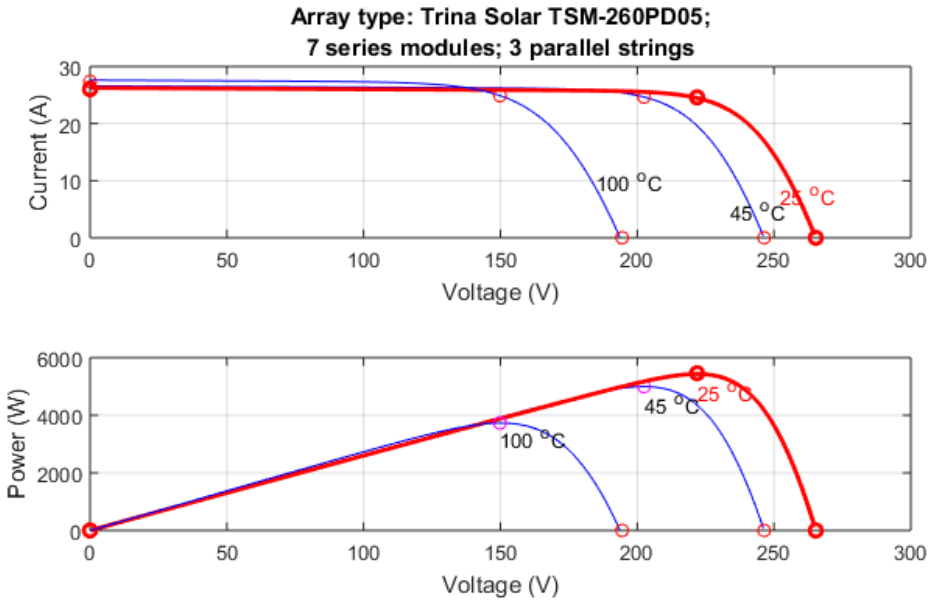

Fig. 13. Current and power curves of the simulated PV array with cell temperature. Source: own elaboration.

The simulation model in *Simulink*® was based on the one presented in [55], and available in the *"Simscape Power Systems"* package of the *Simulink*® sample library. Fig. 14 shows the block diagram of the implemented model, where in the top raw, the first block simulates the PV field array, the second a DC/DC converter which implements the increment inductance MPPT integral controller, third is the DC bus which models the power link with the BESS. Finally, fourth block is an AC/DC bidirectional inverter and the last block simulates the power load demand. On the bottom raw, the first block represents the BESS through a parametrized battery model, while the second block is a DC/DC bidirectional converter. All voltage converters have been modelled considering a conversion efficiency over 90% and include PWM controllers.

A controllable power load has been added to simulate the power delivery limitation when it exists. This load is controlled by a power switch commanded by an MPPT stabilizer according to the BESS response and that can be seen in detail in Fig. 15. As it can be seen in this figure, to keep the MPPT controller of the PV inverter stable, the load disconnection was associated with a 1 ms holder at the time of connection of the battery system. On the other hand, Fig. 16 shows the configuration of the BESS controller, where upstream flank stepped pulses were used in the battery power to avoid permanent oscillations around the tripping values.

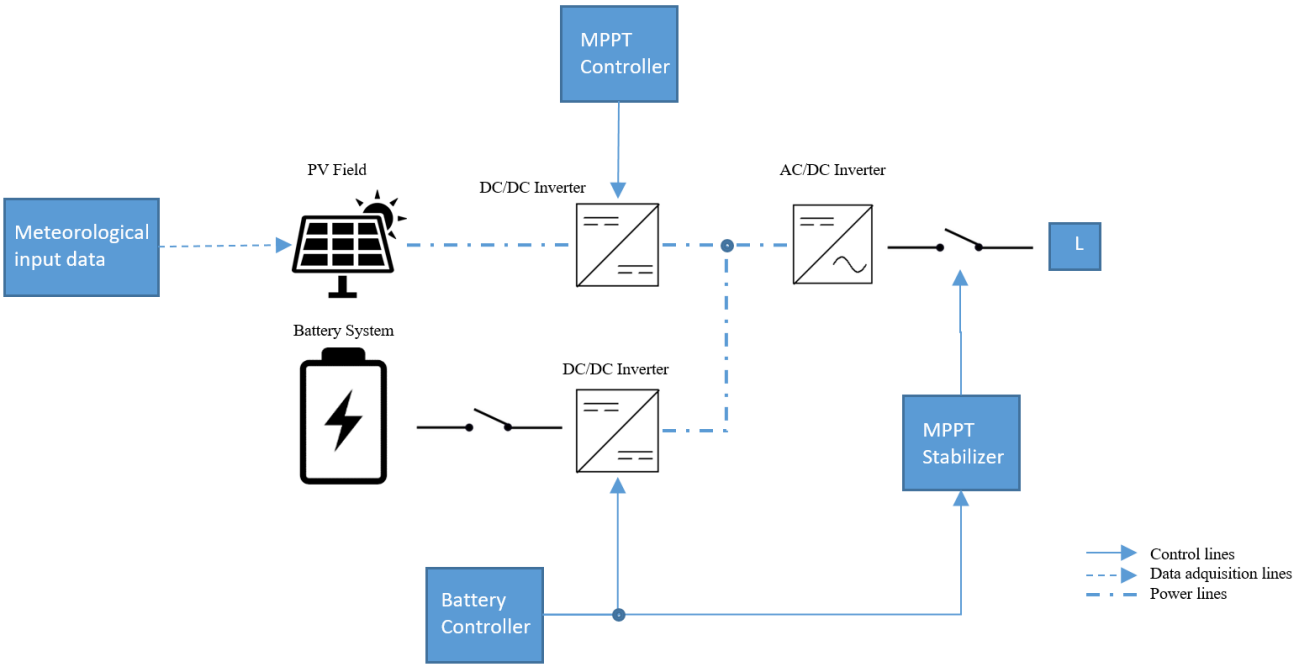

Fig. 14. *Simulink*® PV generation with BESS on DC bus model. Source: own elaboration.

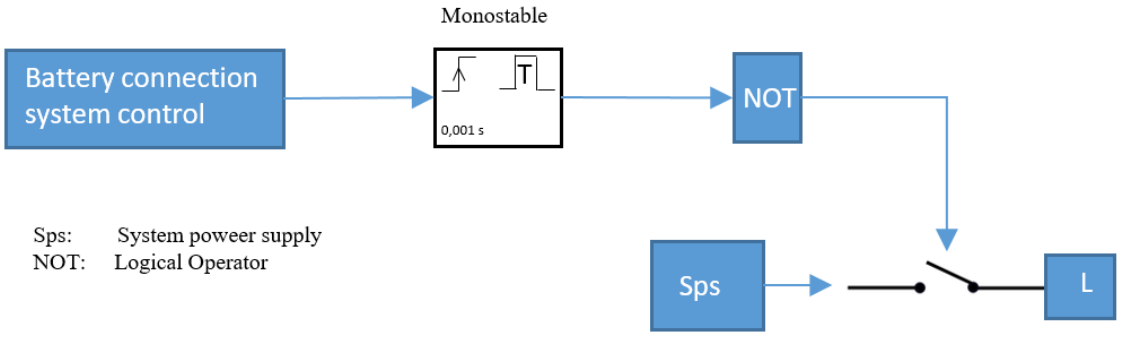

Fig. 15. MPPT stabilizer for BESS connection and power delivery limitation simulation. Source: own elaboration.

All the blocks employed in the simulation have been designed considering technical specifications as voltage range operation, input output power and efficiencies. The whole system has been designed considering the efficiency on each scenario, meaning the energy consumed on the reduced load due to considering the global efficiency for the whole system.

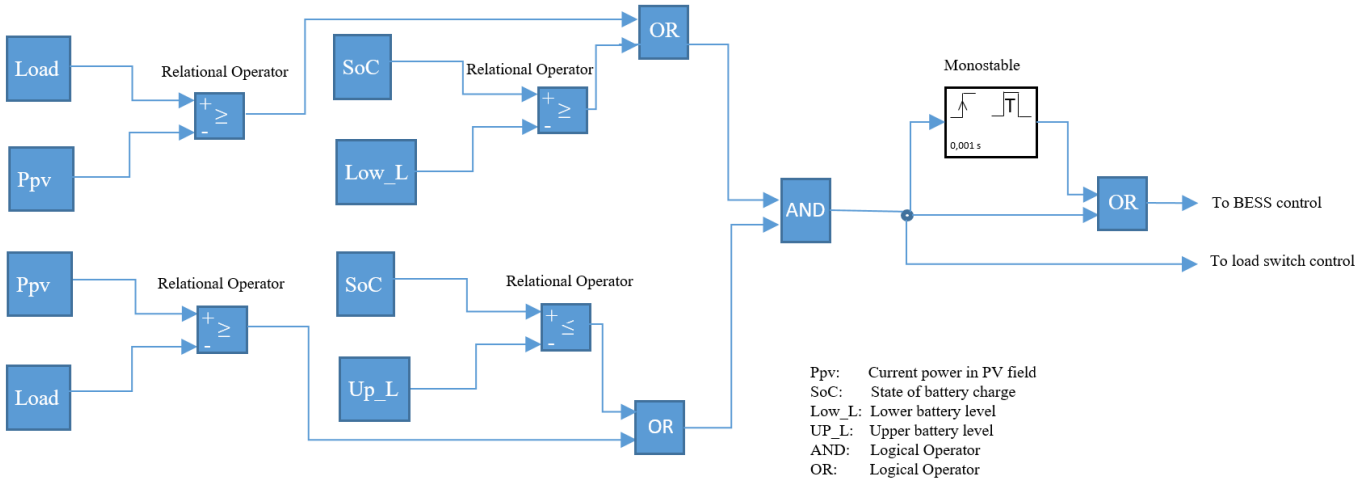

Fig. 16. BESS controller system. Source: own elaboration.

As it can be seen in Fig. 16, the BESS controller system operates in such a way that, when the PV power exceeds the limit, the surplus will be sent to the batteries. On the other hand, when the PV power is not sufficient to supply the load, the shortage will be complemented with available battery charge. If there is not enough capacity in the batteries, the priority will be to supply the load. This procedure is achieved by the simulation using inverter blocks which implement insulated gate bipolar transistor or IGBTs, whose trigger doors are controlled by pulse width modulated signals (PWM). The BESS controller is linked to BESS DC/DC bidirectional converter.

Table 3 summarizes the descriptions of all the components used to model the system.

Table 3. Model components description. Source: own elaboration.

Component	Type	Description
PV module	Model block	*Simulink*® library block. Fed by input data files.
DC/DC converter	Model block	*Simulink*® library block. DC converter based on IGBTs.
DC bus	Model block	*Simulink*® library block. DC bus for components connections.
DC/AC converter	Model block	*Simulink*® library block. DC/AC converter based on IGBTs.
Battery	Model block	*Simulink*® library block. Li-ion model.
PWM	Model block	*Simulink*® library block. Pulse width modulator.
MPPT	Algorithm	*Simulink*® library Algorithm. MPPT inverter controller.
Battery controller	Algorithm	*Simulink*® library Algorithm. Battery controller.
Load control	Model block	*Simulink*® self-defined block. Model load supply and battery control.
Stabilizer control	Model block	*Simulink*® self-defined block. MPPT model stabilization control.
Input data	External file	Radiation and temperature input data.

As the integration step in the model must be T_{sample} = 5 µs, at the most, in order to keep the model stable, every second of simulation was considered as one hour of real time. Then, the BESS installed capacity and operation frequency must be scaled accordingly. Therefore, a scaled equivalent capacity for the BESS has been considered in the model 3,600 times smaller (as 1 kW·s in the simulation represents 1 kW·h in the real system). Considering the optimum capacity to be 4 kWh in the represented *Simulink*® system, simulated BESS size has to be set to 1.1 Wh. Moreover, bearing in mind that the *Simulink*® battery model has a nominal voltage of 200 V_{dc} and a current capacity of 40 Ah, the resulting storage capacity of 8 kWh must be scaled. Hence, in order to simulate the optimal BESS size, the equivalent SOC percentage variation will be 0.014% in the model. The BESS starts from a 79.32% SoC.

Finally, Fig. 17 shows three samples of the traces corresponding to the three different PWM signals involved in the simulation. Subfigure (a) represents the PWM control signals of the implemented BESS controller being BESS signal 1 the controller of the series IGBT and BESS signal 2 the controller of the parallel IGBT, subfigure (b) the PWM pulses of the DC/DC power converter (output of the MPPT controller), and subfigure (c) includes the PWM signals of the 4 IGBTs for the voltage conversion from DC to AC in the single-phase inverter.

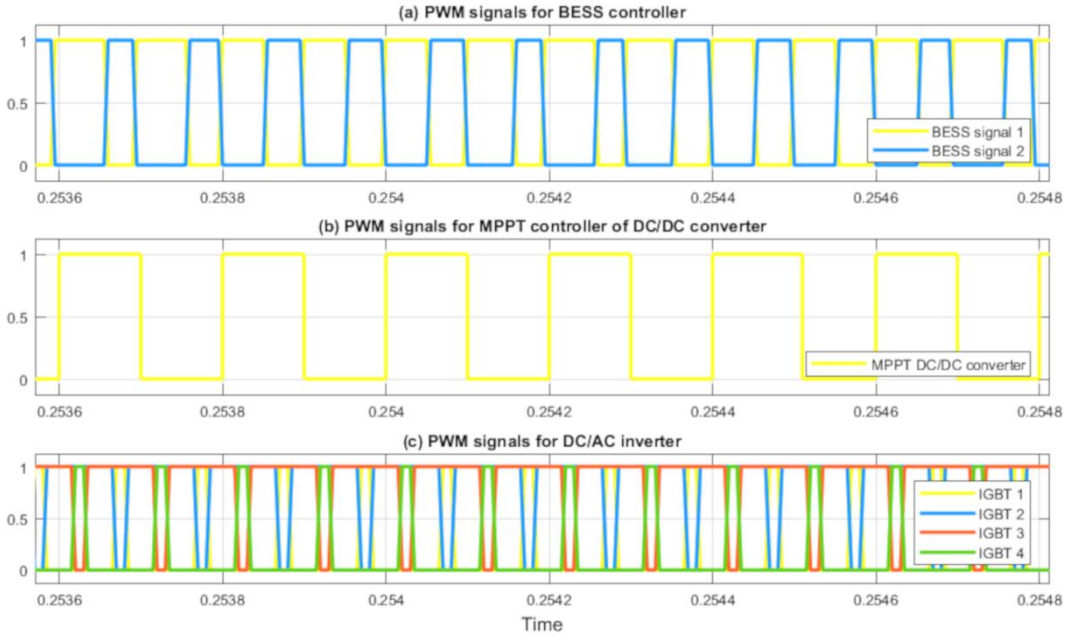

Fig. 17. Simulated PWM traces: (a) BESS controller, (b) DC/DC power converter and (c) DC/AC power inverter. Source: own elaboration.

Three representative radiation days were chosen to run the simulation scenarios, including only daylight hours. Input data files were average hourly irradiance and ambient temperature values which are linearly interpolated in the simulation. A total of 49 real time hours have been simulated including one very low radiation conditions day, one average radiation conditions day and high radiation conditions day. On the other hand, variables evolution during the simulation are registered by employing scope tools from the *Simulink*® libraries.

Once that the simulations have been properly configured, a first simulation without BESS is run in order to verify the model. In this scenario, all generated power is injected and accepted by the external power grid. Therefore, power loads and BESS were removed from the model. However, the bi-directional power inverter, the DC bus circuit with a snubber circuit, and the harmonic and choke filters were maintained in the model. Moreover, the MPPT controller was replaced by the one developed in [52].

Then, three BESS scenarios were simulated. Scenario 1 includes the optimal calculated BESS size (4.12 kWh for the *Simulink*® case), while scenarios 2 and 3 implement double the optimal calculated BESS size and the half of the optimal size, respectively. Figures in Appendix A show the simulation results (power values and main parameters values) while Table 4 summarizes the parameter values achieved for each scenario considering the three representative days simulated in a row.

Table 4. Simulink model parameters results. Source: own elaboration.

Scenario	**BESS size [kWh]**	**Δ SoC [%]**	**Power delivery limit [kW]**	$C_{achievement}$ **[%]**	C_{extra} **[%]**	**f(C,L) [-]**
1 (opt)	4.12	0.014	2	57.06	97.71	0.5575
2 (double)	8.00	0.028	2	29.20	100	0.2920
3 (half)	2.00	0.007	2	64.12	54.89	0.3519

The results provide evidence that the surplus energy coefficient (C_{extra}) is approximately 100% for scenario 1 and exactly 100% for scenario 2, meaning that the optimal calculated BESS size allows the minimization of curtailed energy. On the other hand, the achievement coefficient ($C_{achievement}$) is significantly higher in the first scenario than in the second one. Moreover, the third scenario with BESS size being the half of the calculated optimum shows a slightly better value for the achievement coefficient than the first scenario but very low C_{extra} value, meaning a very reduced capacity to recover curtailed energy (especially during the third simulation reference day).

Appendix A shows the results of the simulation of the three proposed scenarios, showing both BESS power, PV generation power (Figs. A1, A3 and A5) and power load curves, and BESS voltage, current and SoC (Figs. A2, A4 and A6. In the first set of figures, positive power values mean energy injected to the power grid while negative power values mean surplus energy stored by the BESS.

Furthermore, each one of the three graphs which are shown on each figure in the appendix show three different parts corresponding to the three simulated irradiance conditions (reference days).

It must be remembered that the power load curve (third graph in Figs. A1, A3 and A5) simulates a constant power load set at 2 kW which must be fed from the generated solar PV power and the BESS system if necessary and it represents the power delivery limitation to the external power grid. When the available generation power (sum of the PV power and the BESS power) is below this limitation, the power load is adjusted to the generation power value.

On the other hand, it must be noticed that BESS current and SoC curves in Figs. A2, A4 and A6 show opposite evolutions noting that discharging currents are considered positive and charging currents negative.

Looking into the graphs in the top of Figs. A1, A3 and A5 it can be seen that the BESS is fully charged/discharged (a BESS cycle is completed) for the first and second reference days, but for the third one, BESS available capacity it is not enough to absorb all the generation surplus and then, some energy is curtailed.

From the total solar PV generation potential of 55 kWh for the three simulation days, considering a power grid delivery limitation of 2 kW, the proposed optimal BESS size (4 kWh) is able to recover up to 15.5 kWh of potential curtailed energy due to power delivery limitations, which means an efficiency improvement of 28.18% of the initial solar PV power plant without energy storage.

Finally, the implemented *Simulink*® model in this paper has been also validated with real measurements at the laboratories of the Electrical and Electronic Engineering Department (DIEE) of the Spanish National University for Distance Education (UNED). Found discrepancies with the computer simulations laid within a 3.5% margin of error, which means that simulations have been conducted with high accuracy. Found differences can be attributed to some secondary simplifying assumptions adopted within the model formulation.

5. DISCUSSION

According to the proposed optimization method, it was found that for a real PV power plant, with an installed rated power of 10.2 MW, and with a delivery limitation up to a nominal power of 7.5 MW, the optimal BESS capacity value must be 6.6 MWh. Bearing in mind that a capacity of 2 MWh was initially considered by the power plant owners, it outstands the significant difference between both proposed BESS sizes. However, results show that considering 6.6 MWh of nominal BESS capacity size allows to reach an extra energy injected to the grid up to 1.5-fold during the expected useful lifespan of the power plant, considering that an average use of around 50% is technically acceptable for the use of the BESS capacity.

As shown in the Results section, there is a difference of around 6% between the extra production calculated by means of the proposed optimal design and that calculated as the difference between the two simulated scenarios

(with and without power delivery limitation). This deviation can be understood as a consequence of the fitting curves when abrupt variations occur. It should therefore be noted at this point that there is a limitation to the procedure adjustment to estimate production curves with abrupt variations, limited by the maximum suitable polynomial degree. For abrupt changing external conditions scenarios, discrete integration methods are then preferable.

Although for March, August and November monthly production deviations can be observed between the real measurements and the simulation results (due to *Meteonorm*® provides averaged and normalized irradiation data, which is not strictly achieved when just a single year of measurements are considered), the results are considered representative as the simulations provide good fitting values in the higher production months (when the BESS will be mainly required).

It should be remarked that the proposed method is restricted to power export limitations and, therefore, it is not applicable in those cases in which the scope of a BESS is different, e.g., in those cases where the aim is to provide an isolated installation of PV solar energy with a required degree of autonomy. In this case, the calculation would be obtained by simply estimating daily consumption and the required days of autonomy. On the other hand, the presented method is feasible for the optimal design of self-consumption systems without needs of a net surplus compensation tariff, e.g., PV power plants with a constant power load demand profile during the central hours of the day (12 h range), which want to adapt the typical bell shape of the PV generation to the rectangular shape of the power demand profile.

As stated in the Introduction section, a wide literature for optimal BESS sizing can be found, however the power delivery limitation approach is not commonly considered. In [34], an algorithm is provided to determine a BESS capacity value that minimizes the operating costs of a PV power plant, defined load, BESS, and grid characteristics. Similarly, in [56] an algorithm is provided for an optimal microgrid operation. However, these systems work in such a way that, if the power supply system fails to satisfy the load demand (considering the PV generation and the available energy in the BESS), the system will purchase the necessary energy from the external power grid. If there is a power surplus, it will be stored in the BESS with the possibility to sell it during the most convenient rate period. The procedure designs an algorithm that aims to find a unique critical value of the battery size such that the total cost of the system remains the same if the battery size is larger than or equal to the selected value, and the cost is strictly larger if the battery size is smaller than that needed for the selected capacity value. A similar study is performed in [57], where the specific regulation frame of Germany is considered, and the system is analysed from an economical point of view. A new approach to find the optimal size is presented in [58], where multiple scenarios are analysed with different PV power and BESS capacities looking for the one that minimal electricity costs presents. The procedure proposed in this paper considers an overall system achievement coefficient that interacts in the calculation of optimal capacity. Furthermore, given its easiness, it is highly adaptable to any scenario and hence exportable.

Barsali [36] provides a probabilistic method for the sizing a BESS aimed at improving the integration of PV and V2G systems into the public grid which guarantees (from a statistical point of view) the operation of the grid within acceptable voltage and frequency levels in those cases in which possible investments are conditioned by government initiatives. Our work starts out from the idea of generating an expectation of a rapid return on investment and generation of profit, regardless of government initiatives, and it is based on the already existing feed-in tariff. In [59], a sizing calculation method is established for a specific case on the island of Reunion, obtaining a MWh to MWp ratio that minimizes the difference between the accumulated capacity and the deviation originated by PV production and load demand. It thus seeks to approximate the BESS capacity at the value that makes PV production meet load demand. In [60] the BESS location is analysed for saving grid load peaks. The scope is to avoid equipment grid oversizing; the system will work in order to meet the load with the generation. In our case, we seek a value that maximizes the extra energy obtained conditioned by high achievement, without considering the existing grid load, which is considered as an unlimited capacity.

6. CONCLUSIONS

The main objective of this paper is to provide an optimization tool for sizing BESS capacity for RES (solar PV in the proposed scenarios) when power delivery limitations exist. It has been proved that the developed software tools in VBA predict actual PV power plant behaviour accurately enough and the calculated optimal BESS capacity fulfils established criteria. Moreover, it may be concluded that installing BESS extra capacity allows to reduce curtailed energy and a 30% more energy can be injected yearly to the power grid, although it implies a 15% reduction in the achievement coefficient.

The BESS operation has been moreover validated by *Simulink*® based simulations, where the BESS capacity size fulfils the expectations regarding the maximization of the defined objective function when the proposed method is applied. Therefore, it is evidenced that the optimized capacity provides the minimization of the curtailed energy, maintaining an achievement coefficient high enough (which indirectly optimizes the system costs and the BESS operation conditions). Thus, the BESS capacity sizing following the proposed method allows to provide the maximum energy recovered without the need of an excessively oversized storage system, which is the main innovation of this work and which is worth of interest of RES power plant owners and designers.

It should be noted that the target function can be adapted to other technical or economic criteria. Moreover, the proposed method will serve as the basis for the analysis of the economic model of this sort of power plants, where the installation of a BESS is planned to improve production and increase profits.

According to the findings reported in the Simulations and Results section, for a power plant with completely different parameters from the one used to describe the method, it has been proved that the calculated optimum capacity fits perfectly the target conditions in the three simulated. It hence follows that the method is exportable to different sizes and operating facilities.

Although an economic analysis taking into maintenance costs, the energy sales prices, a detailed investment costs analysis or LCOE evaluation has been reserved for future works, the proposed key factors C_{extra} and $C_{achievement}$ allows a feasible comparison of different BESS installations. Other related proposed research works are: the development and implementation of other integration techniques with better performance under abrupt changing irradiation conditions, hardware implementation of the BESS controller, implementation of adaptive control for BESS with load management capabilities or the analysis of the potential benefit of using BESS for reduced AC rated power installations.

Finally, the main advantages and disadvantages of the proposed method are summarised in Table 5.

Table 5. Main advantages and disadvantages of the proposed optimal BESS size method. Source: own elaboration.

Advantages	Disadvantages
The calculation method can be applied to systems of any topology.	The method is intended to optimize BESS size under power grid delivery limitations.
Fully customizable and configurable.	It should be managed by experts in *Microsoft Excel*® and *PVsyst*® software, or their equivalents.
Specific software (involving high economic costs) are not needed.	The optimization is strictly technical and does not consider economic criteria directly.
It is affordable not only from common PV power plants design software, such as *Microsoft Excel*® and *PVsyst*® software, but also for any other with similar features.	The method is not provided in a *"all in one"* software pack, and need to be implemented with multiple software platforms.
The method allows to perform the main basis criteria to calculate the optimal BESS independently to the RES generation type.	

APPENDIXES

Appendix A. Simulink model results.

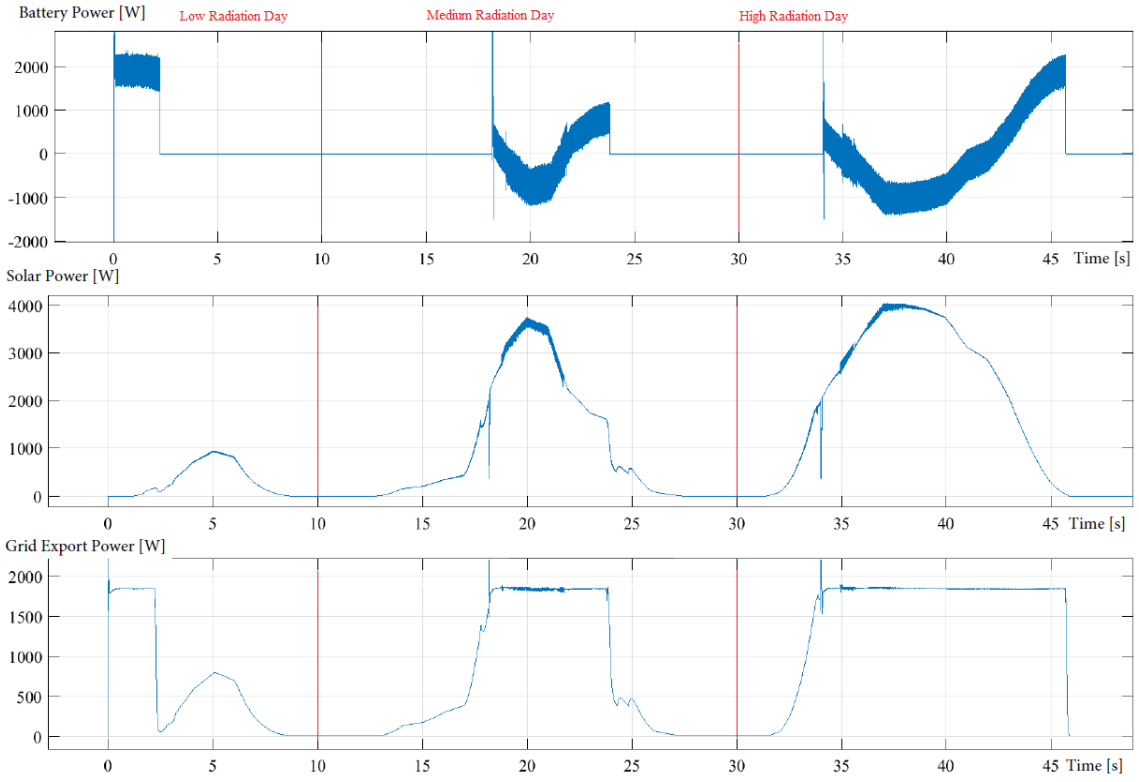

Fig. A1. Simulation results of power evolution in the optimum scenario. Source: own elaboration.

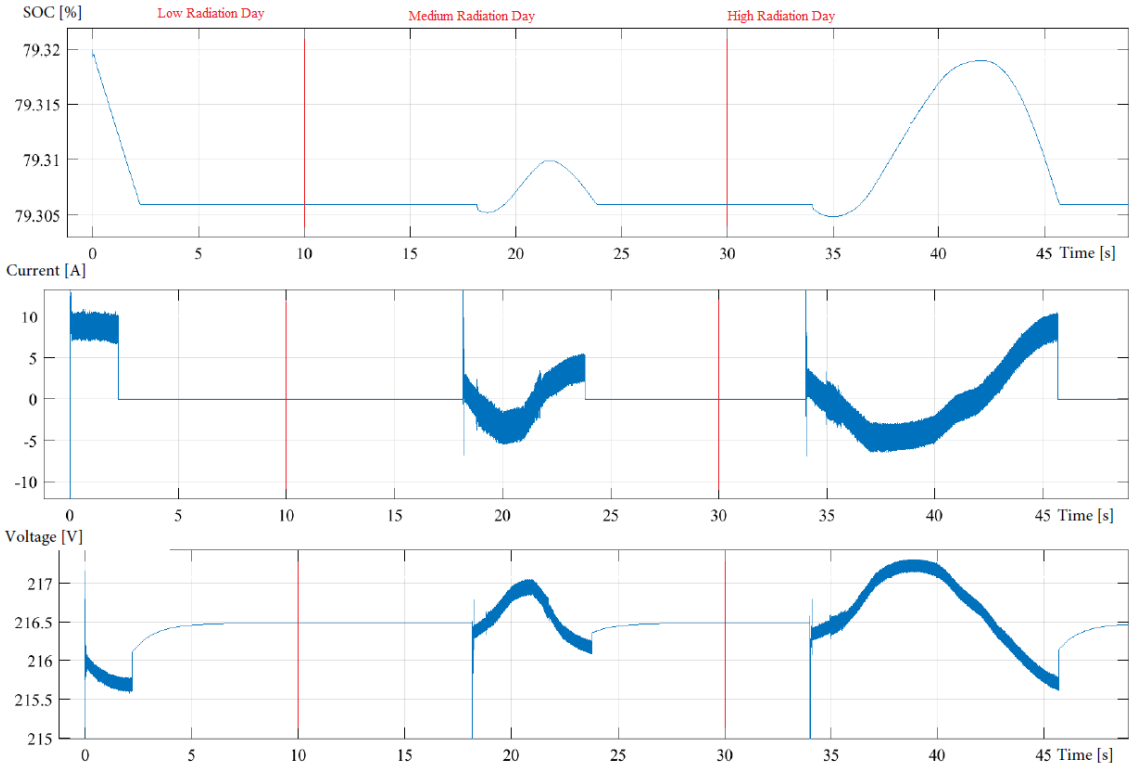

Fig. A2. Simulation results of the evolution of the main battery values in the optimum scenario. Source: own elaboration.

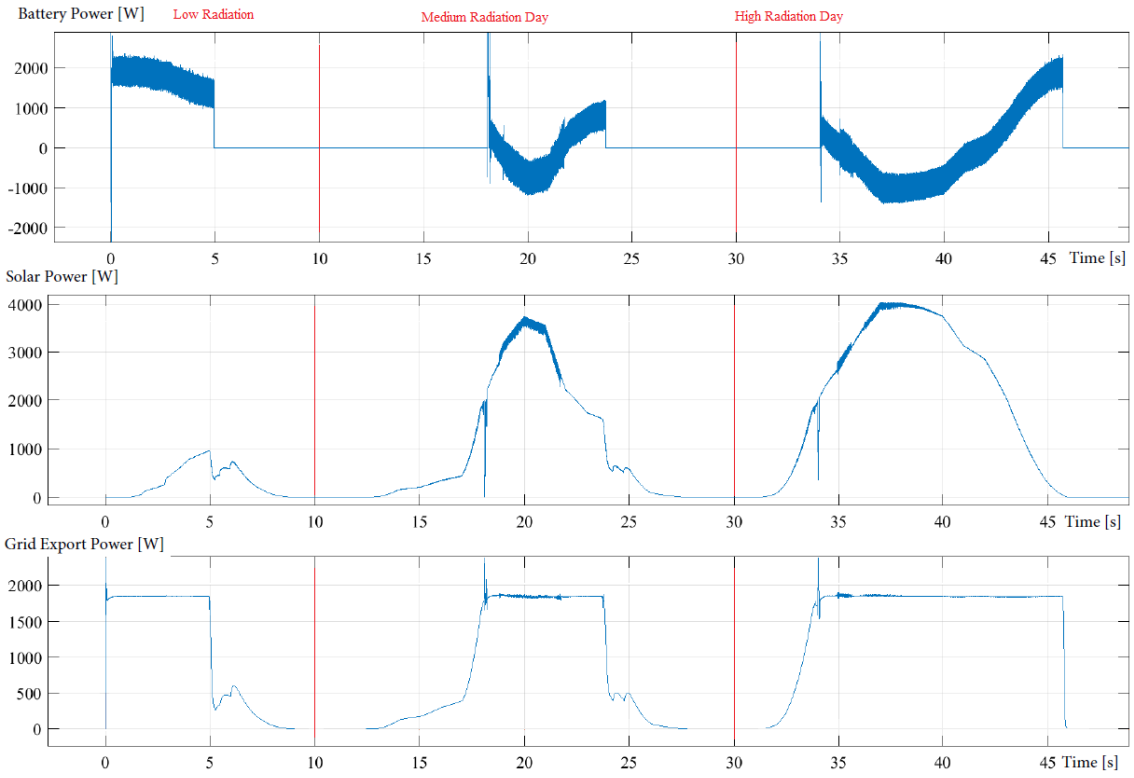

Fig. A3. Simulation results of power evolution in the double-optimum scenario. Source: own elaboration.

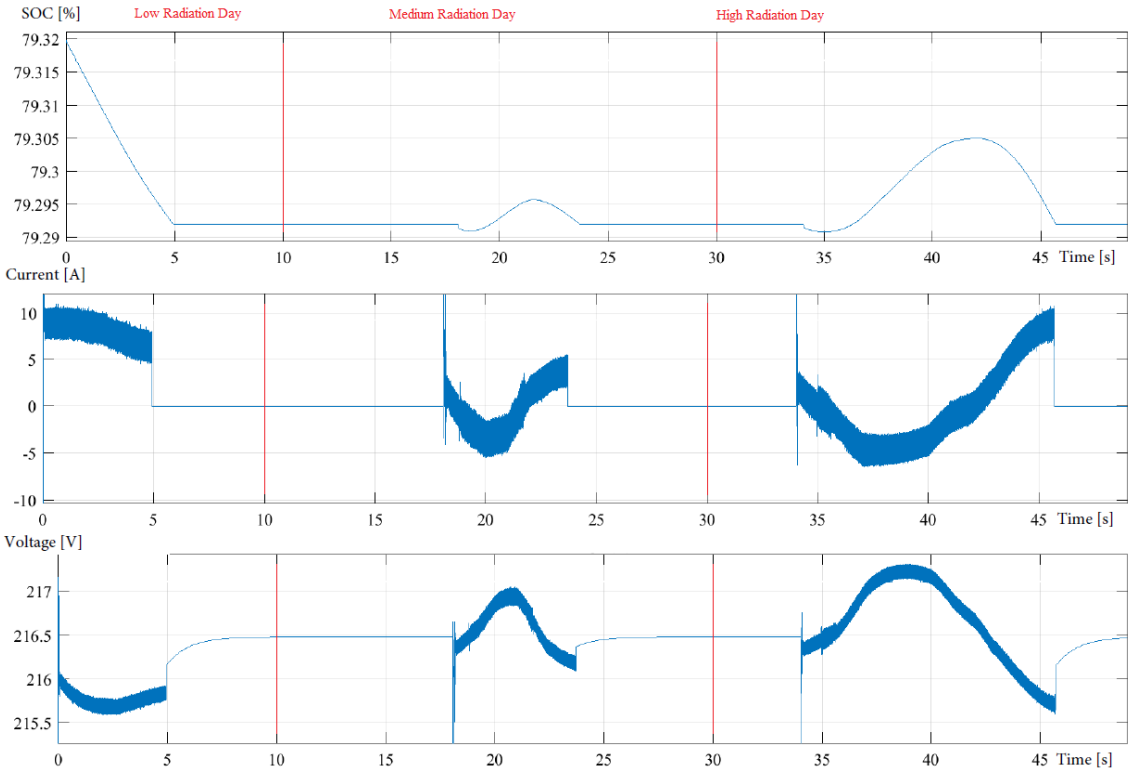

Fig. A4. Simulation results of the evolution of the main battery values in the double-optimum scenario. Source [34]

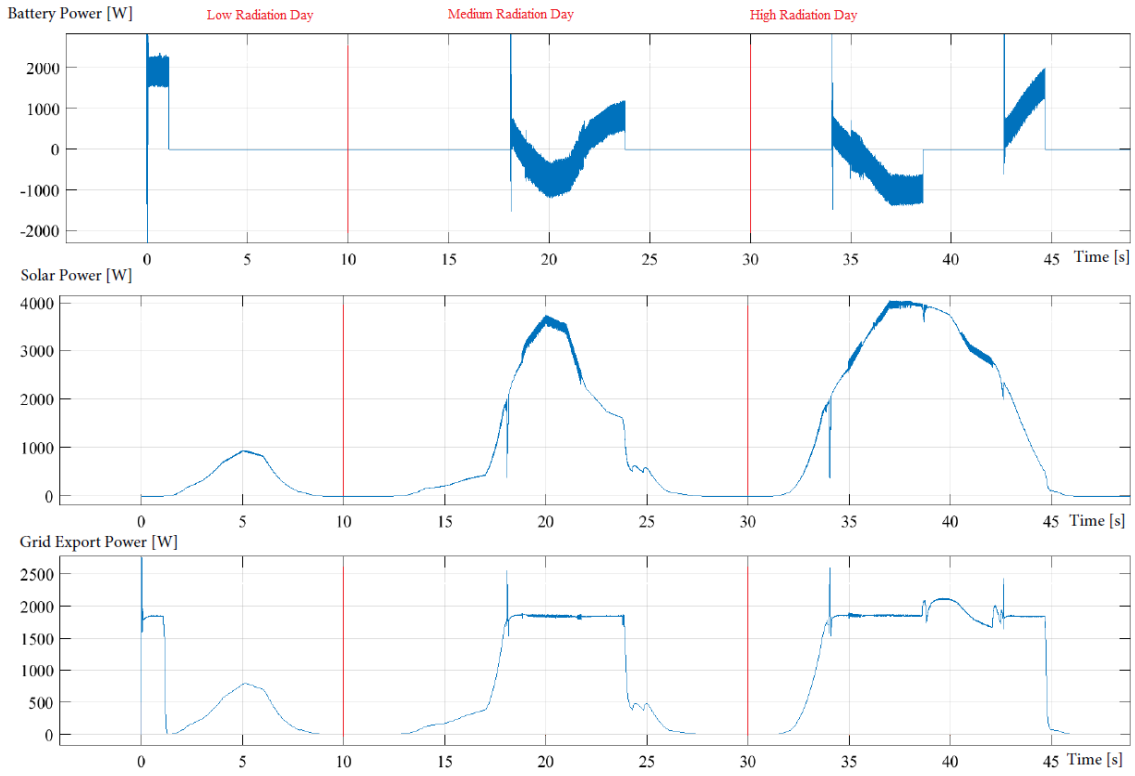

Fig. A5. Simulation results of power evolution in the half-optimum scenario. Source: own elaboration.

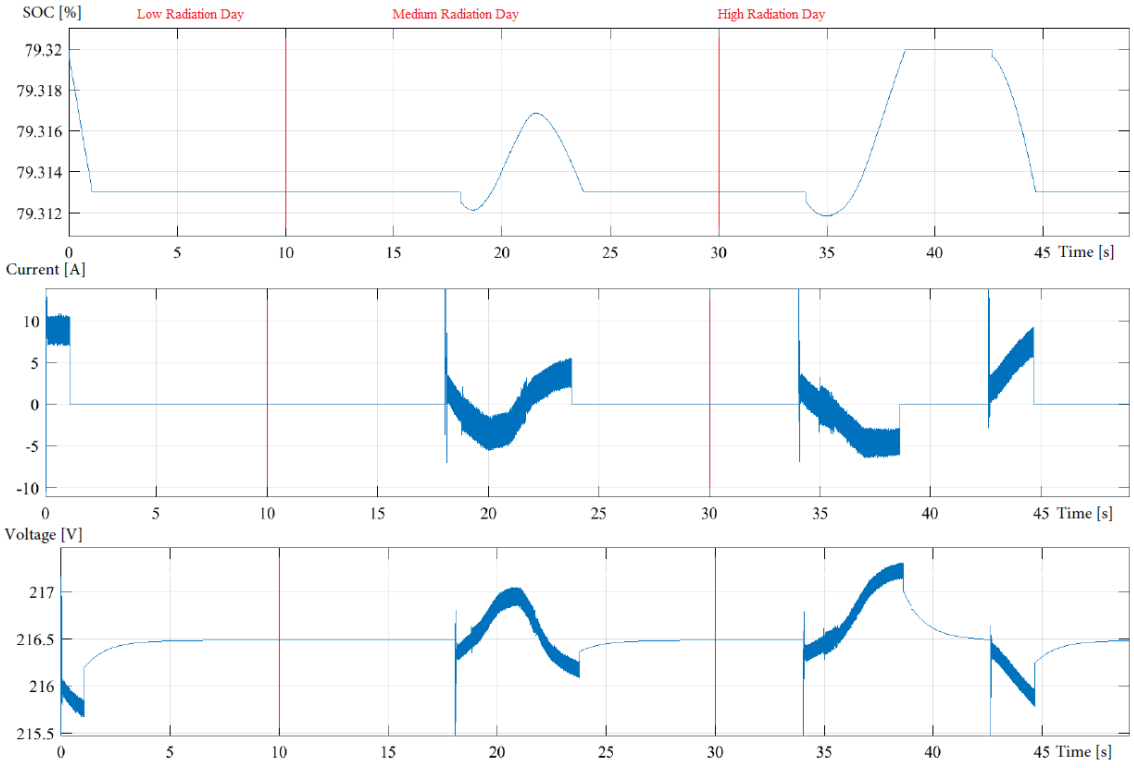

Fig. A6. Simulation results of the evolution of the main battery values in the half-optimum scenario. Source: own elaboration.

ACKNOWLEDGEMENTS

The authors acknowledge the support of UNED´s School of Industrial Engineers for the funding received for the research project in e-learning through the Call for Aid to support Teaching and Research Activities of the Departments of the School in the 2017 Call.

REFERENCES

[1] Royal Decree 1663/2000, of 29 September, about on connection of photovoltaic installations to the low voltage network. 2000

[2] Alsharif MH. Optimization design and economic analysis of energy management strategy based on photovoltaic/energy storage for heterogeneous cellular networks using the HOMER model. Solar Energy 2017;147:133-150

[3] Ross M, Hidalgo R, Abbey C, Joós G. Analysis of Energy Storage Sizing and Technologies. IEEE Electrical Power & Energy Conference 2010

[4] Tarroja B, Zhang L, Wifvat V, Shaffer B, Samuelsen S. Assessing the stationary energy storage equivalency of vehicle-to-grid charging battery electric vehicles. Energy 2016;106:673–690

[5] Luo Y, Zhu T, Wan S, Zhang S, Li K. Optimal charging scheduling for large-scale EV (electric vehicle) deployment based on the interaction of the smart-grid and intelligent-transport systems. Energy 2016;97:359–368

[6] Goli P, Shireen W. FV powered smart charging station for PHEVs. Renewable Energy 2014;66:280–287

[7] Yahiaoui A, Fodhil F, Benmansour K, Tadjine M, Cheggaga N. Grey wolf optimizer for optimal design of hybrid renewable energy system PV-Diesel Generator-Battery: Application to the case of Djanet city of Algeria. Solar Energy 2017;158:941-951

[8] Yahyaoui I, Atieh A, Tadeo F, Tina GM. Energetic and economic sensitivity analysis for photovoltaic water pumping systems. Solar Energy 2017;144:376-391

[9] Mennoud A. PVsyst ® Version 5.55 [software]. 2013 Feb 21 [cited 2014 May 1]. Available from: http://www.pvsyst.com/.

[10] Little JN, Moler C, Bangert S. MATLAB 9.1. Version R2016b [software]. 2016 Sep 1 [cited 2016 Nov 13]. Available from: https://es.mathworks.com/MATLAB

[11] Barcia, L.A.; Peon, R.; Díaz, J.; Pernía, A.; Martínez, J.Á. Heat Transfer Fluid Temperature Control in a Thermoelectric Solar Power Plant. Energies 2017, 10, 1078.

[12] Dolara, A.; Grimaccia, F.; Magistrati, G.; Marchegiani, G. Optimization Models for Islanded Micro-Grids: A Comparative Analysis between Linear Programming and Mixed Integer Programming. Energies 2017, 10, 241.

[13] Muñoz-Cruzado-Alba, J.; Rojas, C.A.; Kouro, S.; Galván Díez, E. Power Production Losses Study by Frequency Regulation in Weak-Grid-Connected Utility-Scale Photovoltaic Plants. Energies 2016, 9, 317.

[14] Andika R, Kim Y, Yoon SH, Kim DH, Choi JS, Lee M. Techno-economic assessment of technological improvements in thermal energy storage of concentrated solar power. Solar Energy 2017;157:552-558

[15] Jayasekara N, Wolfs P, Masoum M. An optimal management strategy for distributed storages in distribution networks with high penetrations of PV. Electric Power Systems Research 2014;116:147–157.

[16] Syed I M, Raahemifar K. Energy advancement integrated predictive optimization of photovoltaic assisted battery energy storage system for cost optimization. Electric Power Systems Research 2016 (Article in Press)

[17] Kollera M, Borscheb T, Ulbigb A, Anderssonb G. Review of grid applications with the Zurich 1 MW battery energy storage system. Electric Power Systems Research 2015;120:128–135

[18] Hung D Q, Mithulananthan N, Bansal RC. Integration of PV and BES units in commercial distribution systems considering energy loss and voltage stability. Electric Power Systems Research 2014;113:128–135

[19] Reihani E, Sepasi S, Roose L R, Matsuura M. Energy management at the distribution grid using a Battery Energy Storage System (BESS). Electrical Power and Energy Systems. 2016;77:337–344

[20] Heydari A, Askarzadeh A. Techno-economic analysis of a PV/biomass/fuel cell energy system considering different fuel cell system initial capital costs. Solar Energy 2016;133:409-420

[21] Shukla AK, Sudhakar K, Baredar P. Design, simulation and economic analysis of standalone roof top solar PV system in India. Solar Energy 2016;136:437-449

[22] Thalange VC, Dalvi VH, Mahajani SM, Panse SV, Joshi JB. Deformation and optics based structural design and cost optimization of cylindrical reflector system. Solar Energy 2017;158:687-700

[23] Ratnam EL, Weller SR, Kellett CM. An optimization-based approach to scheduling residential battery storage with solar FV: Assessing customer benefit. Renewable Energy 2015;75:123–134

[24] Lorenzi G, Santos Silva C A. Comparing demand response and battery storage to optimize self-consumption in PV systems. Applied Energy 2016;180:524–535

[25] Eghtedarpour N, Farjah E. Control strategy for distributed integration of photovoltaic and energy storage systems in DC micro-grids. Renewable Energy 2012;45:96–110

[26] Reihani E, Ghorbani R. Load commitment of distribution grid with high penetration of photovoltaics (FV) using hybrid series-parallel prediction algorithm and storage. Electric Power Systems Research 2015;131:224–230

[27] Torreglosa JP, García P, Fernandez LM, Jurado F. Energy dispatching based on predictive controller of an off-grid wind turbine/photovoltaic/hydrogen/battery hybrid system. Renewable Energy 2015;74:326–336

[28] Nottrott A, Kleissl J, Washom B. Energy dispatch schedule optimization and cost benefit analysis for grid-connected, photovoltaic-battery storage systems. Renewable Energy 2012;55:230–240

[29] Mulder G, Six D, Claessens B, Broes T, Omar N, Van Mierlo J. The dimensioning of PV-battery systems depending on the incentive and selling price conditions. Applied Energy 2013;111:1126–1135

[30] Rodrigues EMG, Godina R, Santos SF, Bizuayehu AW, Contreras J, Catalnao JPS. Energy storage systems supporting increased penetration of renewables in islanded systems. Energy 2014;75 265–280

[31] Amirante R, Cassone E, Distaso E, Tamburrano P. Overview on recent developments in energy storage: Mechanical, electrochemical and hydrogen technologies. Energy Conversion and Management 2017;132 372–387

[32] Cervone A, Carbone G, Santini E, Teodori S. Optimization of the battery size for FV systems under regulatory rules using a Markov-Chains approach. Renewable Energy 2016;85:657–665

[33] Jia H, Mu Y, Qi Y. A statistical model to determine the capacity of battery–supercapacitor hybrid energy storage system in autonomous microgrid. Electrical Power and Energy Systems 2014;54:516–524

[34] Ru Y, Kleissl Y, Martinez S. Storage Size Determination for Grid-Connected Photovoltaic Systems. IEEE transactions on sustainable energy 2013;4(1):1949–3029

[35] Bracale A, Caramia P, Carpinelli G, Mancini E, Mottola F. Optimal control strategy of a DC micro grid. Electrical Power and Energy Systems 2015;67:25–38

[36] Nozahya MSE, Abdel-Galila TK, Salama MMA. Probabilistic ESS sizing and scheduling for improved integration of PHEVs and FV systems in residential distribution systems. Electric Power Systems Research 2015;125:55–66

[37] Barsali S, Ceraolo M, Giglioli R, Poli D. Storage applications for Smartgrids. Electric Power Systems Research 2015;120:109–117

[38] Zalani Daud M, Mohamed A, Hannan M A. An improved control method of battery energy storage system for hourly dispatch of photovoltaic power sources. Energy Conversion and Management 2013;73:256–270

[39] German Federal Ministry for Economy and Energy Law for the development of renewable energies (Law of Renewable Energies EEG 2014). 2014.

[40] Spanish Ministry for Economy. Royal Decree 436/2004, of 12 March, establishing the methodology for updating and systematizing the legal and economic activity of electricity production with special fee. 2004.

[41] Italian Authority for the Electricity Gas and Water, Resolution 522/14/R/eel. Provisions for the dispatching of non-predictable renewable sources in response to the decision of the Council of State. Section 2014.-9 Friday, June 2014, n. 2936.

[42] OFGEM. Renewables obligation (RO). 2015. [accessed 20.12.16] URL: https://www.ofgem.gov.uk/environmental-programmes/renewables-obligation-ro.

[43] Delfanti M, Falabretti D, Merlo M. Energy storage for PV power plant dispatching. Renewable Energy 2015;80:61–72

[44] Puerto Rico Authority for the Electrical Energy. Government of Puerto Rico. Manuals, Regulations and Other (web host). San Juan: 2016 [accessed 03.01.17] URL: http://www.prepa.com/spanish.asp?url=http://www.aeepr.com/Servicios/manuales.asp

[45] Lund H, Andersen AN, Østergaard PA, Mathiesen BV, Connolly D. From electricity smart grids to smart energy systems e A market operation based approach and understanding. Energy 2012;42:96–102

[46] Aghamohammadi M R, Abdolahinia H. A new approach for optimal sizing of battery energy storage system for primary frequency control of islanded Microgrid. Energy 2014;54:325–333

[47] BYD Company Limited. BYD Energy Storage Solutions (sede web). Pingshan: BYD Company Limited; 2013 [accessed 20.12.16] URL: http://www.byd.com/energy/ess.html.

[48] Power Electronics, S.L. Freesun PPC (web host). Paterna: 2017 [accessed 07.01.17] URL: http://power-electronics.com/es/inversoressolares/accesorios/freesun-ppc/.

[49] Meteotest. Meteonorm ® Software (web host). Bern: [accessed 20.12.16] URL: http://www.Meteonorm.com.

[50] PHOTON Consulting. Photon.info (web host). Andover: 2016 [accessed 20.12.16] URL: http://www.photon.info/en.

[51] S Anuphappharadorn, S Sukchai, C Sirisamphanwong, N Ketjoy. Comparison the economic analysis of the battery between lithium-ion and lead-acid in PV stand-alone application. Energy Procedia 2014;56:352–358

[52] De Brito MAG, Sampaio LP, Luigi Jr. G, Guilherme A, Melo C, Canesin A. Comparative Analysis of MPPT Techniques for PV Applications 2011; International Conference on Clean Electrical Power (ICCEP).

[53] Trina Solar Limited. PC05A Peoduct, Honey Series (web host). Changzhou: 2016 [accessed 20.12.16] URL: http://2016.trinasolar.com/sp/product/Mu_Honey.html.

[54] Samil Power Co., Ltd. SAMIL POWER Expert for PV Gried-tied inverters (web host). Suqian: 2016 [accessed 20.12.16] URL: http://www.samilpower.com/.

[55] The MathWorks, Inc. MATLAB examples (web host). Natick: 2017 [accessed 20.12.16] URL: https://es.mathworks.com/examples/simpower/mw/sps_product-power_HEMS-home-energy-management-system#2.

[56] Bahmani-Firouzi B, Azizipanah-AbarghooeeVR. Optimal sizing of battery energy storage for micro-grid operation management using a new improved bat algorithm. Electrical Power and Energy Systems 2014;56:42–54

[57] Linssen J, Stenzel P, Fleer J. Techno-economic analysis of photovoltaic battery systems and the influence of different consumer load profiles. Applied Energy 2017;185:2019–2025

[58] Bortolini M, Gamberi M , Graziani A. Technical and economic design of photovoltaic and battery energy storage system. Energy Conversion and Management 2014;86:81–92

[59] Bridier L, David M, Lauret P. Optimal design of a storage system coupled with intermittent renewables. Renewable Energy 2014;67:2–9

[60] Yunusov T, Frame D, Holderbaum W, Potter B. The impact of location and type on the performance of low-voltage network connected battery energy storage systems. Applied Energy 2016;165:202–213